Title: Viral-mediated Oct4 overexpression and inhibition of Notch signaling synergistically induce neurogenic competence in mammalian Müller glia.

Authors: Nguyet Le [1†], Sherine Awad[6-8†], Isabella Palazzo[1], Thanh Hoang[6-8], Seth Blackshaw[1-5*]

1 Department of Neuroscience,
2 Department of Ophthalmology,
3 Department of Neurology,
4 Institute for Cell Engineering,
5 Kavli Neuroscience Discovery Institute,
Johns Hopkins University School of Medicine, Baltimore, MD 21205
6 Department of Ophthalmology and Visual Sciences, University of Michigan School of Medicine, Ann Arbor, MI 48105
7 Department of Cell and Developmental Biology, University of Michigan School of Medicine, Ann Arbor, MI 48105
8 Michigan Neuroscience Institute, University of Michigan School of Medicine, Ann Arbor, MI 48105
[†]These authors contributed equally.
*To whom correspondence should be addressed.

Abstract: Retinal Müller glia in cold-blooded vertebrates can reprogram into neurogenic progenitors to replace neurons lost to injury, but mammals lack this ability. While recent studies have shown that transgenic overexpression of neurogenic bHLH factors and glial-specific disruption of NFI family transcription factors and Notch signaling induce neurogenic competence in mammalian Müller glia, induction of neurogenesis in wildtype glia has thus far proven elusive. Here we report that viral-mediated overexpression of the pluripotency factor *Oct4* (*Pou5f1*) induces transdifferentiation of wildtype mouse Müller glia into bipolar neurons and stimulates this process synergistically in parallel with Notch loss of function. Single cell multiomic analysis shows that *Oct4* overexpression leads to widespread changes in gene expression and chromatin accessibility, inducing activity of both the neurogenic transcription factor Rfx4 and the Yamanaka factors Sox2 and Klf4. This study demonstrates that viral-mediated overexpression of Oct4 induces neurogenic competence in wildtype retinal Müller glia, identifying mechanisms that could be used in cell-based therapies for treating retinal dystrophies.

Introduction: The homeodomain factor Oct4 (Pou5f1) is a central component of transcriptional regulatory networks that maintain pluripotency in embryonic stem (ES) cells. Along with Sox2, Klf4, and Myc, Oct4 is one of the Yamanaka factors sufficient to induce the formation of induced pluripotent stem cells (iPSCs) from virtually all somatic cell types (Takahashi and Yamanaka 2006). In contrast to these other factors, *Oct4* is selectively expressed in ES cells and essentially absent from somatic cells, including adult stem cells from every tissue examined. The two clear exceptions are found in gonadal stem cells (Takashima et al. 2013; Uhlen et al. 2010) and during neural crest formation, where *Oct4* expression is essential for the ability of these cells to generate diverse cell types (Zalc et al. 2021; Morrison

and Brickman 2006). This has raised the question of whether *Oct4* overexpression *in vivo*, alone or in combination with other pluripotency factors, may confer some level of multipotency on somatic cells in the central nervous system.

Sustained overexpression of the Yamanaka factors *Oct4*, *Sox2*, *Klf4,* and *Myc* induces teratoma formation, depending on the tissues targeted (Ohnishi et al. 2014; Abad et al. 2013). Transient or low-level Yamanaka factor overexpression, in contrast, has been reported to induce cellular rejuvenation in both neurons and other cell types (Ocampo et al. 2016; C. Wang et al. 2021), although this occurs without clear induction of proliferation or conferring multipotency. However, several studies have directly investigated whether sustained viral-mediated overexpression in CNS neural stem or glial cells of Oct4 alone, or in combination with subsets of other pluripotency factors, can induce multipotency and neurogenesis. Results from these studies are mixed, with *Oct4* overexpression in neural stem cells reported to either not induce neurogenesis (Asadi et al. 2015; Samaneh Dehghan et al. 2015; Sim et al. 2011), to promote formation of oligodendrocyte progenitors (OPCs) (Yu et al. 2021), or to promote remyelination in committed OPCs (S. Dehghan et al. 2016). Two studies reported that viral-mediated *Oct4* overexpression, either alone (Niu et al. 2013) or in combination with other Yamanaka factors (Gao et al. 2016), could directly convert reactive astrocytes into neurons. However, these studies used the GFAP minipromoter to drive gene expression, which has been reported to show ectopic insert-dependent silencing in glia and activation in neurons (L.-L. Wang et al. 2021). This limitation makes these findings difficult to interpret, as alternative methods of validating cell lineage were not used.

In the retina, two studies have reported injury-dependent induction of *Oct4* in Müller glial cells in zebrafish and mice. In zebrafish, where injury induces Müller glia to undergo conversion to neurogenic progenitors (Wan and Goldman 2016), it was claimed that *Oct4* is essential for glial reprogramming to occur (Sharma et al. 2019). In mice, where neurogenic competence is rapidly and actively suppressed following injury, it was reported that *Oct4* expression is transiently induced, but fully repressed within 24 hours following injury (Reyes-Aguirre and Lamas 2016). This raises the possibility that *Oct4* expression may be sufficient to confer neurogenic competence on retinal Müller glial cells. In this study, we assessed whether AAV-mediated overexpression of Oct4 could induce reprogramming of adult mouse Müller glia. While we did not detect any expression of *Oct4* in either zebrafish or mouse Müller glia following injury, we use both genetic cell lineage and single-cell omics analyses to unambiguously demonstrate that viral-mediated overexpression of *Oct4* is sufficient to induce the formation of bipolar neurons from wildtype mouse Müller glia. We further show that *Oct4* overexpression synergistically enhances existing levels of Müller glia-derived neurogenesis in the absence of Notch signaling, partly by facilitating transcription of neurogenic bHLH factors. This represents the first report in which a virally-delivered construct induces direct conversion of mammalian Müller glia into retinal neurons *in vivo*.

Results:

Oct4 and other pluripotency factors are not detectably expressed in Müller glia or Müller glia-derived progenitor cells in either zebrafish or mice

To examine the expression of *Oct4* and other pluripotency-associated genes in both wildtype and neurogenic Müller glia, we analyzed bulk and single-cell RNA-Seq data previously generated by our group from zebrafish and mice (Hoang et al. 2020). Consistent with previous findings (Nelson et al. 2011; Surzenko et al. 2013), we detected robust expression of *Sox2* and *Klf4* in both resting and injured Müller glia from both species (Fig. S1a,b). However, we did not detect any expression of *Oct4* or its direct target *Nanog* (Loh et al. 2006). Similarly, we did not observe any induction of *Oct4* in snRNA-Seq data from mouse Müller glia made neurogenic by selective loss of function of *Rbpj* alone or in combination with *Nfia/b/x* (Le et al. 2024) (Fig. S1c). These results indicate that injury does not induce detectable levels of *Oct4* mRNA or its direct pluripotency-associated targets in Müller glia.

AAV-mediated overexpression of *Oct4* induces conversion of wildtype mouse Müller glia to bipolar-like cells

To determine whether *Oct4* overexpression could reprogram mammalian Müller glia into a neurogenic state, we administered intraperitoneal tamoxifen injections into P21 *GlastCreER;Sun1-GFP* mice to irreversibly label Müller glia with Sun1-GFP (Hoang et al. 2020; de Melo et al. 2012) (Fig. 1a). One week following the final tamoxifen injection, we performed intravitreal injections of either Gfap-Oct4-mCherry 7m8 AAV or Gfap-mCherry control. While neurogenic bHLH factors expressed using these vectors were rapidly silenced in Müller glia and activated in amacrine and retinal ganglion cells, we found that Gfap-Oct4-mCherry remained selectively expressed in Müller glia, but did not induce detectable levels of Müller glia-derived neurogenesis in the uninjured retina (Le et al. 2022). We next tested whether excitotoxic injury could induce neurogenic competence in wildtype Müller glia transfected with Gfap-Oct4-mCherry. To do this, we performed an intravitreal injection of N-methyl-d-aspartate (NMDA) to induce excitotoxic injury and reactivity (Hoang et al. 2020) one week post-viral injection. We then administered EdU for one week immediately after NMDA injection to label proliferating cells. Retinas were harvested and analyzed 5 weeks following NMDA injection (Fig. 1b).

Immunostaining analysis revealed enriched mCherry expression in Müller glia in both control mCherry and Oct4-mCherry infected retinas (Fig. 1C). In addition, Oct4 expression was enriched in GFP-positive Müller glia in Oct4-mCherry infected retinas but not in mCherry control retina (Fig. S2a). We also observed selective expression of the neurogenic bHLH factor Ascl1 in Oct4-mCherry infected Müller glia (Fig. S2b). While Sun1-GFP-positive cells infected with Oct4-mCherry mostly express the Müller glial marker Sox2 (Fig. S2c, white arrows), a subset of GFP-positive cells did not show detectable Sox2 expression (Fig. S2c, yellow arrows). Furthermore, while Sun1-GFP expression was only detected in Müller glia in mCherry-infected retinas, we observed that 5.1% of GFP-positive cells co-localized with the bipolar cell marker Otx2 in Oct4-mCherry infected retinas (Fig. 1c,d). Immunostaining of additional cell-specific markers showed that a subset of these GFP-positive cells expressed the cone bipolar markers Scgn and Cabp5 (Fig. S2d,e), but did not express either the rod and cone ON bipolar cell marker Isl1 or the rod marker Nrl (Fig. S2f,g). We did not observe any expression of the amacrine cell marker HuC/D (Fig. 1c,d), which is observed in neurons generated from neurogenic mouse Müller glia that are deficient for either *Rbpj* or *Nfia/b/x* (Hoang et al. 2020; Le et al. 2024). We likewise did not observe any GFP-positive cells incorporating 5-ethynyl-2'-deoxyuridine (EdU) (Fig.S2h),

indicating that Oct4 overexpression in wildtype Müller glia did not induce proliferation. Taken together, these findings show that viral-mediated *Oct4* overexpression is sufficient to directly transdifferentiate wildtype adult mouse Müller glia into retinal bipolar-like cells.

Oct4 overexpression synergistically enhances glial-derived neurogenesis induced by genetic disruption of Notch signaling

In our previous study, we found that disrupting Notch signaling in adult mouse Müller glia, either by selective deletion of the transcriptional effector *Rbpj* or by combined disruption of *Notch1* and *Notch2*, induces transdifferentiation into bipolar and amacrine-like cells (Le et al. 2024). To further characterize the effects of *Oct4* overexpression in the absence of Notch signaling, we first used *GlastCreER;Rbpj*$^{lox/lox}$*;Sun1-GFP* mice to genetically label Müller glia while disrupting *Rbpj* function (Fig. 2a). We then performed intravitreal injection of either control or *Oct4* overexpression constructs, followed by NMDA and EdU injection as performed for *GlastCreER;Sun1-GFP* mice. Retinas were collected 5 weeks following NMDA treatment (Fig. 2b). Immunostaining confirmed selective expression of Oct4 protein in GFP-positive Müller glia of Oct4-mCherry infected retinas, but not in mCherry-infected controls (Fig. S2i). We observed that many GFP-positive cells in Oct4-mCherry-infected retinas did not express the Müller glial marker Sox9 (Fig. S2j, yellow arrows), which suggests that they have lost their glial identity.

Five weeks following NMDA injury, we observed 4.5% of GFP-positive cells in retinas of mCherry-infected controls expressed the bipolar cell marker Otx2, while 0.7% expressed the amacrine cell marker HuC/D (Fig. 2c,d). These levels of neurogenesis are consistent with previous findings in uninfected retinas (Le et al. 2024). In contrast, we observe 24.3% of GFP-positive cells expressing Otx2 in Oct4-mCherry-infected retinas, representing a significant ($p < 0.0001$) increase relative to control. However, we did not observe a significant change in the relative fraction of GFP/HuC/D-double-positive cells. As observed in wild-type retinas, no EdU incorporation was detected in Oct4-expressing Müller glia (Fig. S2k), indicating that the observed neurogenesis is due to direct transdifferentiation of Müller glia into retinal neuron-like cells, rather than through reprogramming to a proliferative neuronal progenitor-like state.

Next, we tested whether Oct4 overexpression could further enhance neurogenesis in other cell-specific mutants that induce neurogenic competence in adult Müller glia. We have previously observed Müller glia-specific *Notch1/2* double mutants phenocopy neurogenesis seen in Rbpj mutants (Le et al. 2024). To do this, we used *GlastCreER;Notch1*$^{lox/lox}$*;Notch2*$^{lox/lox}$*;Sun1-GFP* mice (Fig. S3a), and analyzed the effect of Oct4 overexpression using the same protocol previously described for wildtype and *Rbpj* mutants (Fig. S3b). We observed 15.8% of GFP+ Müller glia colocalized with Otx2 in Oct4-mCherry-infected retinas compared to 6.6% GFP/Otx2+ cells in samples infected with control mCherry vector (Fig. S3c). Infection with Oct4-mCherry vector induced both Ascl1 (Fig. S3d) and Oct4 (Fig. S3e) expression selectively in *Notch1/2*-deficient Müller glia.

Finally, we also tested whether Oct4 overexpression could enhance Müller glia-derived neurogenesis induced by selective loss of function of the transcription factors *Nfia*, *Nfib*, and *Nfix* (Hoang et al. 2020). *GlastCreER;Nfia*$^{lox/lox}$*;Nfib*$^{lox/lox}$*;Nfix*$^{lox/lox}$*;Sun1-GFP* mice (Fig. S4a)

were infected with both mCherry and Oct4-mCherry vectors as previously described, and harvested at 5 weeks following NMDA infection (Fig. S4b). However, we observed only very limited coexpression of mCherry and GFP following infection with either construct (Fig. S4c), indicating that NFI factors may be required for appropriate glial-specific expression of the GFAP minipromoter construct, as suggested by previous studies in astrocytes (Cebolla and Vallejo 2006).

Oct4 overexpression promotes expression of reactive glial markers and neurogenic bHLH factors

To gain insight into the mechanism by which Oct4 stimulates neurogenesis in *Rbpj*-deficient Müller glia, we conducted single-cell (sc)RNA-Seq analysis of GFP-positive cells FACS-isolated from retinas of *GlastCreER;Rbpj*$^{lox/lox}$*;Sun1-GFP* mice infected with either GFAP-mCherry control or GFAP-Oct4-mCherry virus. Retinas were tamoxifen- and NMDA-treated as described in Figure 2, and GFP-positive cells isolated at 8 weeks following NMDA treatment (Fig. 3a). We profiled 12,143 GFP+ cells from control-infected and 14,612 GFP+ cells from Oct4-mCherry-infected retinas (Fig. 3b). In both samples, we observe a clear differentiation trajectory connecting Müller glia, neurogenic Müller glia-derived progenitor cells (MGPCs), and differentiating amacrine and bipolar cells (Fig. 3b). Oct4-infected retinas consistently show substantially higher fractions of bipolar cells (20.5 % vs. 2.7 %), and a smaller fraction of Müller glia (71.4 % vs. 88.2 %), consistent with immunohistochemical data (Fig. 3c).

Selective molecular markers could readily distinguish Müller glia (*Glul*, *Apoe*, *Vim*, *Clu*, *Rlbp1*) from neurogenic MGPCs (*Neurog2*, *Ascl1*, *Sox4*, *Hes6*, *Dll1*), and clearly identified differentiating bipolar (*Otx2*, *Pcp2*, *Pcp4*, *Car10*, *Gabrb3*) and amacrine-like cells (*Nrxn1*, *Tfap2b*, *Nrg1*, *Snap25*) (Fig. 3d-f, Fig.S5, Table ST1). In both MGs and MGPCs, we observed substantial differences in gene expression between samples infected with control and Oct4-mCherry samples. Oct4-infected Müller glia selectively downregulated genes specific to resting Müller glia (*Car2*, *Dkk3*, *Glul*, *Col23a1, Abca8a*), and upregulated genes enriched in reactive glia (*Gfap*, *Socs3*, *Nupr1*, *Mt1/2/3*, *Fos*, *Jun*, *Klf6*) (Fig. 3e,f, Table ST1). In MGPCs, Oct4 also downregulated both transcription factors (*Lhx2*, *Hopx*) and other genes (*Apoe*, *Dio1*, *Il33*, *Espn*) that are enriched in resting Müller glia, and upregulated many genes selectively expressed in activated glia (*Mt1/2/3*, *Fos*, *Jun*, *Nupr1, Socs3*). In addition, Oct4-infected MGPCs expressed consistently higher levels of neurogenic bHLH factors (*Ascl1*, *Neurog2*, *Hes6*), promote bipolar cell specification (*Otx2*), or otherwise broadly promote neurogenesis (*Insm1*, *Dll3*, *Mybl1*) or are selectively expressed in late-stage neurogenic progenitors in the developing retina (*Gadd45a*, *Btg2*) (Clark et al. 2019) (Fig. 3e,f, Table ST1). These findings imply that Oct4 enhances bipolar cell formation in *Rbpj*-deficient Müller glia potentially by repressing expression of genes that promote quiescence such as *Lhx2* (de Melo et al. 2016, 2018), increasing expression of genes that broadly promote neurogenesis, and selectively increasing expression of the bipolar cell-promoting factor *Otx2* (Chan et al. 2020; S. Wang et al. 2014).

Single-cell multiomic analysis identifies targets of Oct4 in wildtype and *Rbpj*-deficient Müller glia

To further investigate the mechanism by which Oct4 promotes neurogenesis, we conducted simultaneous single-nucleus (sn)RNA-Seq and ATAC-Seq on GFP-positive cells from both wildtype and *Rbpj*-deficient Müller glia infected with either control or Oct4-mCherry vectors at 8 weeks following NMDA injection (Fig. 4a). UMAP analysis of integrated cellular snRNA/ATAC-Seq profiles was then used to identify cell clusters. Müller glia were distributed in essentially separate Müller glia clusters specific to wildtype and *Rbpj*-deficient animals, with MGPCs giving rise to bipolar and amacrine cells (Fig. 4b,c). As expected, *Oct4* overexpression induces formation of small numbers of bipolar cells from wildtype Müller glia, and substantially enhances bipolar cell generation from *Rbpj*-deficient MGPC (Fig. 4d, Fig. S6). Although small numbers of rod and cone photoreceptors are detected in this analysis, their proportions do not substantially change between treatment conditions, and therefore likely represent cellular contaminants.

Oct4 overexpression leads to significant changes in gene expression in both wildtype and *Rbpj*-deficient Müller glia. The transition from resting to neurogenic MGPCs to bipolar cells is associated with downregulation of genes that are specifically expressed in resting Müller glia, including *Aqp4, Hes1, Tcf7l2,* and *Lhx2* (Fig. 4e,f, Table ST2). Motif analysis likewise showed that chromatin accessibility is reduced for target motifs for transcription factors that maintain glial quiescence such as Nfia/b/x and Lhx2 (Fig. 4g, Fig. S6, Table ST2). MGPCs likewise show increased accessibility at Stat1/3 motifs, as well as target motifs for neurogenic transcription factors such as Ascl1, Neurog2, and Neurod1 (Fig. 4g), consistent with previous studies of MGPCs generated from Nfia/b/x and Rbpj-deficient Müller glia (Hoang et al. 2020; Le et al. 2024).

Oct4 overexpression in both wildtype and *Rbpj*-deficient Müller glia clusters respectively induces upregulation of 534 and 1657 genes, while respectively downregulating 439 and 824 genes (Fig. 4h). A total of 156 genes are upregulated in both wildtype and *Rbpj*-deficient Müller glia, while 63 genes are downregulated. In both wildtype and *Rbpj*-deficient Müller glia, Oct4 upregulates multiple classes of ion channels, including mechanosensitive (*Piezo2*), Trp (*Trpm*1, *Trpm3*), and chloride channels (*Clca3a1*, *Clca3a2*), as well as GABA receptors (*Gabra4*, *Gabrb1*), cyclic nucleotide phosphodiesterases (*Pde8b*, *Pde11a*), and the neuropeptide *Npy*. *Oct4* overexpression also selectively downregulates multiple inflammation-associated genes *(B2m*, *H2-D1*), small GTPases (*Gbp2*, *Igtp*, *Irgm2*, *Rab13*, *Rgs20*, *Tgtp2*), along with the glycolytic enzyme *Gapdh* and many ribosomal subunits (Fig. 4h, Table ST3). This functionally diverse range of genes that are not prominently expressed in retinal progenitors, and whose role in controlling neurogenic competence remains to be investigated.

Oct4 also differentially regulates multiple transcription factors in both wildtype and *Rbpj*-deficient Müller glia. As expected, *Pou5f1* mRNA is strongly upregulated (Fig. 4e,h), with increased chromatin accessibility also being observed at the endogenous *Pou5f1* promoter, indicating that Oct4 stimulates its own expression in Müller glia (Fig. 4i, Table ST4). *Oct4* overexpression likewise robustly upregulates both the transcription factor *Rfx4* and accessibility at its endogenous promoter (Fig. 4e,h,i, Table ST4). Overexpression of *Rfx4* is sufficient to induce neurogenesis when overexpressed in human embryonic stem cells (Choi et al. 2024;

Joung et al. 2024). *Rfx4* is not detectably expressed in developing mouse retina (Clark et al. 2019), indicating that Oct4-dependent induction of neurogenesis may occur at least in part by mechanisms other than simply inducing dedifferentiation to a retinal progenitor-like state.

Several other transcription factors are only differentially regulated following *Oct4* overexpression in *Rbpj*-deficient Müller glia. One notable upregulated transcription factor is Klf4, which cooperates with Oct4 to induce pluripotency (Takahashi and Yamanaka 2006). Stat1, in contrast, which inhibits neurogenesis induced by Ascl1 overexpression in Müller glia (Jorstad et al. 2020), is selectively downregulated in *Rbp*j-deficient Müller glia (Fig. 4h, Table ST3).

Analysis of changes in chromatin accessibility induced by Oct4 reveals that the consensus motif for Oct4 and its close variant Pit1 (Pou1f1) show the strongest increase in accessibility, followed by Rfx family motifs (Fig. 4j,Table ST5). Both wildtype and *Rbpj*-deficient MG show increased accessibility associated with Sox2, which directly interacts with Oct4 and cooperates to induce pluripotency (Rizzino 2013). While Oct4 does not significantly upregulate the pluripotency factor *Klf4* in wildtype Müller glia, it robustly induces *Klf4* expression *Rbpj*-deficient Müller glia, and likewise selectively induces accessibility at Klf4 consensus motif sites (Fig. 4j). In addition, *Rbpj*-deficient Müller glia also show smaller but still significant increases in accessibility at target sites for the proneural factor Neurog2 and the neurogenic factor Insm1 (Lyu et al. 2021), identifying additional mechanisms by which Oct4 might synergistically enhance neurogenesis (Fig. 4j, Table ST5).

Discussion:

In this study, we demonstrate that AAV-mediated overexpression of Oct4 is sufficient to induce neurogenic competence in wildtype Müller glia in adult mice, and to synergistically enhance neurogenesis induced by genetic disruption of Notch signaling. Oct4 overexpression does not induce proliferation or a general dedifferentiation to a retinal progenitor-like state but instead promotes direct glia-to-bipolar cell transdifferentiation by simultaneously upregulating expression of neurogenic bHLH factors and the bipolar cell promoting factor *Otx2*. Additionally, Oct4 upregulates expression of the neurogenic transcription factor Rfx4, which is not expressed during retinal development, and accomplishes this in part by broadly increasing chromatin accessibility at predicted regulatory sites associated with these genes.

While we do not detect endogenous Oct4 expression in either resting or neurogenic Müller glia, the fact that these cells express robust levels of *Sox2* and *Klf4* implies that they may already be particularly susceptible to partial reprogramming induced by Oct4. Our results contrast with two previous reports, which originally motivated us to carry out this work. A previous study in zebrafish showed weak levels of the Oct4 homolog *pou5f3* in resting glia, with these levels increasing dramatically following injury and reported detecting *pou5f3* expression using qRT-PCR, immunoblotting, and *in situ* hybridization (Sharma et al. 2019). We remain unclear as to why we were unable to detect pou5f3 expression in zebrafish Müller glia in any of the many bulk and single-cell RNA-Seq samples we profiled (Hoang et al. 2020). We also did not detect the previously reported low levels of injury-induced *Oct4* expression in mouse Müller glia (Reyes-Aguirre and Lamas 2016), as these were detected using qRT-PCR, which can

detect extremely low levels of transcript. Similar discrepancies in observed cellular patterns of expression have been observed in many other tissues (Lengner, Welstead, and Jaenisch 2008), and further work will be needed to clarify these discrepancies.

This study represents the first case where viral expression coupled with genetic cell lineage analysis was convincingly used to induce conversion of adult mammalian Müller glia to retinal neurons. Previous studies have reported that *Ascl1* overexpression can do this, but only in immature Müller glia (P11) (Pollak et al. 2013). One other study reported efficient conversion of Müller glia to photoreceptors using a complex cocktail of overexpressed factors, including *Ctnnb1*, *Otx2*, *Crx*, and *Nrl* (Yao et al. 2018), while another reported efficient conversion of Müller glia to retinal ganglion cells following overexpression of *Atoh7* and *Pou4f2* (Xiao et al. 2021). However, these studies both used GFAP minipromoters to both drive expression of these constructs and to infer cell lineage. Multiple studies have shown that GFAP minipromoter specificity is heavily influenced by insert sequences present in AAVs, which can result in both silencing of expression in glia and ectopic activation of expression in neurons (L.-L. Wang et al. 2021; Le et al. 2022). As a result, it cannot be concluded that these represent bona fide glia-to-neuron conversion *in vivo*. Similar claims have been made about knockdown of the RNA binding protein *Ptbp1*, which was variously claimed to directly convert Müller glia to either retinal ganglion cells or photoreceptors, but has been debunked using genetic cell lineage analysis (Hoang et al. 2022; Xie, Zhou, and Chen 2022). In this study, the combination of prospective cell lineage analysis using the *GlastCreER;Sun1-GFP* transgene before infection with GFAP-Oct4-mCherry vector, in combination with scRNA-Seq analysis of infected cells, rules out any potentially confounding factors resulting from the GFAP minipromoter.

Our finding that Oct4 can synergistically enhance neurogenesis induced by genetic disruption of Notch signaling raises the question of whether this might be more broadly applicable to other models of induced neurogenesis in mammalian Müller glia. The mechanism by which Oct4 induces glial-derived neurogenesis appears complex, and to differ fundamentally from that seen following either overexpression of *Ascl1* or loss of function of *Nfia/b/x* and/or *Rbpj* (Hoang et al. 2020; Le et al. 2024; Jorstad et al. 2017). In these cases, Müller glia broadly upregulate proneural genes and/or downregulate Notch signaling. Oct4 instead induces expression of the neurogenic transcription factor *Rfx4*, which is not expressed in developing retina. It is likely that activation of this parallel pathway to neurogenic competence in part accounts for synergistic induction of neurogenesis seen in *Rbpj*-deficient Müller glia.

Other mechanisms enhancing Oct4-dependent neurogenesis in the *Rbpj*-deficient Müller glia may include enhanced induction of *Klf4* expression and increased accessibility at target sites for neurogenic transcription factors such as Ascl1. While *Ascl1* overexpression induces Müller glia-derived neurogenesis in adult mice, this occurs only following treatment with HDAC inhibitors (Jorstad et al. 2017), even though Ascl1 is itself a pioneer factor (Păun et al. 2023). *Oct4* overexpression broadly increases the accessibility of putative cis-regulatory sequences associated with both *Neurog2* and *Insm1*, identifying another potential mechanism of synergy. Transient overexpression of Oct4 could potentially further enhance the neurogenic function of Ascl1, and enhance glial-derived neurogenesis more broadly. This may also be the case for

pathways reported to induce glial reprogramming in other CNS regions, such as *Sox2* overexpression (Niu et al. 2015). Since Oct4 overexpression does not induce detectable levels of proliferation, this reduces the potential oncogenic risk, and may ultimately prove to be relevant for the design of cell-based regenerative therapies for treating retinal dystrophies.

Methods:

Mice

Mice were raised and housed in a climate-controlled pathogen-free facility on a 14/10 h light/dark cycle. Mice used in this study were *GlastCreER;Sun1-GFP*, which were generated by crossing the *GlastCreER* and *Sun1-GFP* lines developed by Dr. Jeremy Nathans at Johns Hopkins (de Melo et al. 2012; Mo et al. 2015), and were obtained from his group. *GlastCreER*;*Rbpj*$^{lox/lox}$*;Sun1-GFP* mice were generated by crossing *GlastCreER;Sun1GFP* with conditional *Rbpj*$^{lox/lox}$ *mice* (JAX #034200).
GlastCreER;*Notch1*$^{lox/lox}$*;Notch2*$^{lox/lox}$*;Sun1-GFP* mice were obtained by crossing *GlastCreER*;*Notch1*$^{lox/lox}$*;Sun1-GFP* and *GlastCreER*;*Notch2*$^{lox/lox}$*;Sun1-GFP* mice. Maintenance and experimental procedures performed on mice were in accordance with the protocol approved by the Institutional Animal Care and Use Committee (IACUC) at the Johns Hopkins School of Medicine.

Intraperitoneal tamoxifen (TAM) Injection

To induce *Cre* recombination, animals at ~3 weeks of age were intraperitoneally injected with tamoxifen (Sigma-Aldrich, #H6278-50mg) in corn oil (Sigma-Aldrich, #C8267-500ML) at 1.5mg/dose for five consecutive days.

NMDA treatment

Adult mice were anesthetized with isoflurane inhalation. Two microliters of 100 mM NMDA in PBS were intravitreally injected using a microsyringe with a 33G blunt-ended needle.

EdU treatment

At 1-week post tamoxifen induction, mice were administered EdU (Abcam, #ab146186) via i.p. injections (150µl of 5mg/ml in PBS) and drinking water (0.3 mg/ml) for 7 consecutive days.

Cloning, production, and intravitreal injection of Adeno-Associated Virus

The Addgene #50473 construct which contains a GFAP promoter was used in this study. The EGFP sequence was replaced by the mCherry sequence. The P2A ribosomal self-cleaving peptide is used to simultaneously express *Oct4* 5′ to the mCherry reporter as a single polypeptide, which is then cleaved to generate *Oct4* and mCherry. The coding sequence of *Oct4* was synthesized by GeneWiz. AAV constructs were packaged into AAV2.7m8 by Boston Children's Hospital Viral Core. Following tam induction, one-month-old GlastCreER;Sun1-GFP mice were intravitreally injected with GFAP AAV constructs using a microsyringe with a 33G blunt-ended needle. The titres and injection volume for each construct are listed in table ST6.

Immunohistochemistry and imaging

Collection and immunohistochemical analysis of retinas were performed as described previously (Hoang et al. 2020). Mouse eye globes were fixed in 4% paraformaldehyde (ElectronMicroscopySciences, #15710) for 4 h at 4°C. Retinas were dissected in 1x PBS and incubated in 30% sucrose overnight at 4°C. Retinas were then embedded in OCT (VWR, #95057-838), cryosectioned at 16 µm thickness, and stored at −20°C. Sections were dried for 30 min in a 37°C incubator and washed 3 × 5 min with 0.1% TritonX-100 in PBS (PBST). EdU labeling was performed by using Click-iT EdU kit (ThermoFisher, #C10340, #C10636) following the manufacturer's instructions. Sections were then incubated in blocking buffer (10% Horse Serum (ThermoFisher, #26050070), 0.4% TritonX-100 in 1x PBS) for 2 h at room temperature (RT) and then incubated with primary antibodies in the blocking buffer overnight at 4°C. Primary antibodies used are listed in table ST7.

Sections were washed 4 x 5 min with PBST to remove excess primary antibodies and were incubated in secondary antibodies in blocking buffer for 2 h at RT. Sections were then counterstained with DAPI in PBST, washed 4 x 5 min in PBST and mounted with ProLong Gold Antifade Mountant (Invitrogen, #P36935) under coverslips (VWR, #,48404-453), air-dried, and stored at 4°C. Fluorescent images were captured using a Zeiss LSM 700 confocal microscope. Secondary antibodies used are listed in table ST6.

Cell quantification and statistical analysis

Otx2/GFP-positive and HuC/D/GFP-positive cells were counted and divided by the total number of GFP-positive cells from a single random whole section per retina. AAV infection efficiencies were calculated by the number of mCherry/GFP-positive cells divided by the total number of GFP-positive cells. Each data point in the bar graphs was calculated from an individual retina. All cell quantification data were graphed and analyzed using GraphPad Prism 10. Two-way ANOVA was used for analysis between 3 or more samples of multiple groups. All results are presented as mean ± SD.

Retinal cell dissociation

Retinas were dissected in fresh ice-cold PBS and retinal cells were dissociated using an optimized protocol as previously described (Fadl et al. 2020). Each sample contains a minimum of 4 retinas from 4 animals of both sexes. Dissociated cells were resuspended in ice-cold HBAG Buffer containing Hibernate A (BrainBits, #HALF500), B-27 supplement (ThermoFisher, #17504044), and Glutamax (ThermoFisher, #35050061).

Single-cell RNA-sequencing (scRNA-seq) library preparation

scRNA-seq were prepared on dissociated retinal cells using the 10X Genomics Chromium Single Cell 3' Reagents Kit v3.1 (10X Genomics, Pleasanton, CA). Libraries were constructed following the manufacturer's instructions and were sequenced using Illumina NextSeq. Sequencing data were processed through the Cell Ranger 7.0.1 pipeline (10X Genomics) using default parameters.

Single-cell Multiome ATAC + GEX sequencing library preparation

scATAC-seq and scRNA-seq were prepared on FACS-isolated GFP-positive cells using the 10X Genomic Chromium Next GEM Single Cell Multiome ATAC + Gene Expression kit following the manufacturer's instructions. Briefly, cells were spun down at 500xg for 5 min, resuspended in 100 µl of ice-cold 0.1x Lysis Buffer, lysed by pipette-mixing 4 times, and incubated on ice for 4 min total. Cells were washed with 0.5 ml of ice-cold Wash Buffer and spun down at 500xg for 5 min at 4°C. Nuclei pellets were resuspended in 10-15 µl Nuclei Buffer and counted using Trypan blue. Resuspended cell nuclei (10-15k) were utilized for transposition and loaded into the 10x Genomics Chromium Single Cell system. ATAC libraries were amplified with 10 PCR cycles and were sequenced on Illumina NovaSeq with ~200 million reads per library. RNA libraries were amplified from cDNA with 14 PCR cycles and were sequenced on Illumina NovaSeq 6000

scRNA-seq data analysis

ScRNA-Seq data were pre-processed using Cellranger v7.1.0 using custom mouse genome mm10 with mCherry and Sun1GFP sequences. The cell-by-genes count matrices were further analyzed using Seurat V5.1.0 (Hao et al. 2024).Cells with RNA counts less than 1000 or greater than 25,000, and number of genes less than 500 or greater than 6000 were filtered out as low-quality cells. Additionally, cells with a mitochondrial fraction of greater than 10% were removed. For data visualization, UMAP was generated using the first 20 dimensions. MG and MGPC cell clusters were subsetted for further analysis. Differential gene expression of mCherry control and Oct4-mCherry groups was performed using "FindAllMarkers" function.

Single-cell Multiomic analysis

For the data processing, raw scRNA-seq and scATAC-seq data were processed with the Cell Ranger software version 2.0.2 specifically using cellranger-arc pipeline for formatting reads, demultiplexing samples, genomic alignment, and generating the cell-by-gene count matrix and the fragments files. Both the cell-by-gene count matrix and the fragments files are the final output from the cellranger-arc pipeline and were used for all downstream analysis.

For the data analysis, scRNA-seq and scATAC-seq were analyzed using Archr version 1.0.2. EnsDb.Mmusculus.v79 and BSgenome.Mmusculus.UCSC.mm10 were used for annotations. The arrow file for each sample was created using the cell-by-gene count matrix and the fragments files output from the cellranger-arc pipeline. To filter poor quality cells, Gex_nGenes greater than 500 and less than 5000 were kept, Gex_nUMI greater than 1000 and less than 15,000 were kept. Also, TSSEnrichment greater than 10 and nFrags greater than 5000 were kept, other cells were deemed of poor quality and were filtered out. Gene expression values from a paired scATAC-seq and scRNA-seq multi modal assay were added to the arrow files using "addGeneExpressionMatrix" function. The LSI dimensionality reduction for both scATAC and scRNASeq was computed and combined using the "addCombinedDims" function. UMAP embedding is calculated using "addUMAP" function and clusters are identified from the reduced dimensions. Marker features were used to annotate clusters.

To get peaks, "addReproduciblePeakSet" function was used to get insertions from coverage files, call peaks, and merge peaks and this step internally used macs software. Then the "addPeakMatrix" function was called to independently compute counts for each peak per cell.

To link peaks to genes, “getPeak2GeneLinks” function was called. The “getMarkerFeatures” function was used to get the differential gene expressions and the differential peaks expressions using the GeneExpressionMatrix and PeakMatrix calculated respectively. Peaks with motifs were annotated using the cisbp motif set using “annotatePeaks.pl” from HOMMER version 4.11 to associate the peaks with nearby genes. Full code used for the analysis is available at https://github.com/SherineAwad/OCT4scRNA-ATAC

Funding: This study was supported by an award from the National Eye Institute (R01EY031685) to S.B., a Stein Innovation Award from Research to Prevent Blindness to S.B., and a Young Investigator grant from Alcon Research Institute to T.H.

Author contributions: N.L. collected and analyzed the bulk of all data presented here. S.A. analyzed single-cell multiomic data, and I.P. assisted in multiomic data. T.H. initiated the study and collected pilot data. S.B. supervised, coordinated, and directed this work. N.L., T.H., and S.B. drafted the manuscript, which all authors edited.

Declaration of interests: S.B. is a co-founder and shareholder of CDI Labs, LLC, and receives support from Genentech.

Data and materials availability: All scRNA-seq, snRNA-seq, and scATAC-seq data described in this study are available at Gene Expression Omnibus under accession number GSE277390.

Figure legends:

Figure 1: AAV-mediated overexpression of *Oct4* induces neurogenesis in injured wild-type mouse Müller glia. (A) Schematic of the transgenic construct used to specifically label MG with Sun1-GFP expression. **(B)** Schematic of the GFAP AAV constructs and experimental workflow. **(C)** Representative images of retinas immunolabeled for GFP, mCherry, Otx2, and HuC/D. White arrowheads indicate GFP-positive MG-derived neurons expressing neuronal markers Otx2 or HuC/D. **(D)** Quantification of mean percentage ± SD of GFP-positive Müller glia-derived neurons expressing either Otx2 or HuC/D. TAM, tamoxifen; ONL, outer nuclear layer; INL, inner nuclear layer; GCL, ganglion cell layer. Scale bar = 50µm.

Figure 2: *Oct4* overexpression enhances neurogenesis in MG-specific *Rbpj* knockout. (A) Schematic of the transgenic constructs used to induce loss of function of *Rbpj* specifically in Müller glia. **(B)** Schematic of the GFAP AAV constructs and experimental workflow. **(C)** Representative images of retinas immunolabeled for GFP, mCherry, Otx2, and HuC/D. White arrowheads indicate GFP-positive MG-derived neurons expressing neuronal markers Otx2 or HuC/D. **(D)** Quantification of mean percentage ± SD of GFP-positive Müller glia-derived neurons expressing either Otx2 or HuC/D. TAM, tamoxifen; ONL, outer nuclear layer; INL, inner nuclear layer; GCL, ganglion cell layer. Scale bar = 50µm.

Figure 3: ScRNA-Seq analysis of MG and MG-derived neurons from Rbpj conditional knockout with Oct4 overexpression. **(A)** Schematic of the scRNA-seq experimental pipeline. **(B)** UMAP plot showing the clustering of GFP-positive cells from retinas infected with GFAP-mCherry and GFAP-Oct4-mCherry AAV constructs. **(C)** Stacked bar plots showing the proportion of cells in each cluster across two sample groups. **(D)** Feature plots highlighting the cluster of Müller glia (*Hes5*), neurogenic MGPCs (*Neurog2, Insm1, Ascl1*), bipolar cells (*Otx2*), and amacrine cells (*Elavl3*). **(E)** Heatmap showing the expression of top differentially expressed genes (DEGs) for *Rbpj*-deficient MG cell cluster from retinas infected with GFAP-mCherry and GFAP-Oct4-mCherry AAV constructs. **(F)** Heatmap showing the expression of top differentially expressed genes (DEGs) for MGPC cell cluster from retinas infected with GFAP-mCherry and GFAP-Oct4-mCherry AAV constructs.

Figure 4: Integrated snRNA/scATAC-Seq analysis of control *and Rbpj*-deficient adult Müller glia with Oct4 overexpression. (A) Schematic of the multiomic scRNA/ATAC-seq experimental pipeline. **(B)** UMAP plot of multiomic datasets showing the clustering of GFP+ cells from control and *Rbpj*-deficient MG from GFAP-mCherry and GFAP-Oct4-mCherry AAV infected retinas. **(C)** UMAP plot showing the identity of cell clusters determined by marker gene expression. **(D)** Stacked bar plots represent the proportion of cells in each cluster across different sample groups. **(E)** Feature plots highlighting the cluster of Müller glia (*Hes1*), neurogenic MGPCs (*Neurog2, Sox4*), bipolar cells (*Otx2*), *Pou5f1*- and *Rfx4*-expressing cells. **(F)** Heatmap showing expression of DEGs along the neurogenesis trajectory. (**G**) Heatmap showing differential motif activity along the neurogenesis trajectory. (**H**) Heatmaps of DEGs between Oct4 and mCherry control in the wild-type and Rbpj-deficient MG cell clusters. Venn diagram showing unique and common DEGs between Oct4 and mCherry control in the wild-type and Rbpj-deficient MG clusters. (**I**) Increased chromatin accessibility regions associated

with Oct4 and Rfx4 loci by Oct4 overexpression in both wildtype and *Rbpj*-deficient Müller glia. (**J**) Top-ranked enriched motifs in increased accessibility chromatin regions induced by Oct4 overexpression in wildtype and *Rbpj*-deficient Müller glia cell clusters.

Figure S1: *Oct4/pou5f3* transcript is not detectably expressed in Müller glia after injury. Expression of pluripotency factors in resting or injured zebrafish (**a**) and mouse retina (**b**) after retinal injury from Hoang, et al. 2020 study and in *Nfia/b/x/Rbpj*-deficient Müller glia (**c**) from Le, et al. 2024.

Figure S2: Immunohistochemical analysis of glial, AAV reporter, and additional molecular markers of MG-derived neurons following *Oct4* transduction in WT and *Rbpj*-deficient MG. (**a**-**h**) Representative images of wildtype retina immunolabeled for GFP, mCherry, and (**a**) Oct4, (**b**) Ascl1, (**c**) Sox2, (**d**) Scgn, (**e**) Cabp5, (**f**) Isl1, (**g**) Nrl, (**h**) EdU. (**i-k**) Representative images of Rbpj cKO retina immunolabeled for GFP, mCherry, and (**i**) Oct4, (**j**) Sox9, (**k**) EdU. ONL, outer nuclear layer; INL, inner nuclear layer; GCL, ganglion cell layer. Scale bar = 50μm.

Figure S3: AAV-mediated overexpression of *Oct4* induces neurogenesis in injured *Notch1/2*-deficient mouse Müller glia. (**a**) Schematic of the transgenic mice used to induce deletion of *Notch1/2* specifically in Müller glia. (**b**) Schematic of the experimental workflow. (**c**) Representative images of retinas immunolabeled for GFP, mCherry, Otx2, and HuC/D. White arrowheads indicate GFP-positive Müller glia -derived neurons expressing neuronal markers Otx2 or HuC/D. Quantification of mean percentage ± SD of GFP-positive Müller glia-derived neurons expressing either Otx2 or HuC/D. TAM, tamoxifen; ONL, outer nuclear layer; INL, inner nuclear layer; GCL, ganglion cell layer. Scale bar = 50μm.

Figure S4: *Oct4* overexpression does not enhance neurogenesis in *Nfia/b/x*-deficient Müller glia because the viral GFAP minipromoter is not active in Müller glia. (**a**) Schematic of the transgenic mice used to induce deletion of *Nfia/b/x* specifically in Müller glia. (**b**) Schematic of the experimental workflow. (**c**) Representative images of retinas immunolabeled for GFP, mCherry, Otx2, and HuC/D. White arrowheads indicate mCherry expression in Sox2+ Muller glia that are not Sun1-GFP+. Quantification of mean percentage ± SD of GFP-positive Müller glia-derived neurons expressing either Otx2 or HuC/D. TAM, tamoxifen; ONL, outer nuclear layer; INL, inner nuclear layer; GCL, ganglion cell layer. Scale bar = 50μm.

Figure S5: ScRNA-Seq analysis of Müller glia-derived neurons from Rbpj-deficient Müller glia following Oct4 overexpression. (a**)** UMAP plot showing GFP-positive cells from retinas infected with GFAP-mCherry and GFAP-Oct4-mCherry AAVs. (**b**) Expression of glial and neuronal markers. (**c**) Top DEGs of different cell types generated by Oct4 overexpression in *Rbpj*-deficient Müller glia.

Figure S6: Pseudotime analysis showing the transition from resting to neurogenic MGPCs to bipolar cells. (**a**) Top DEGs across different retinal cell types. (**b**) Pseudotime

trajectory of neurogenesis from Müller glia to bipolar cells. (**c**) Heatmap showing differential chromatin accessible regions along the neurogenesis trajectory.

Table ST1: ScRNA-Seq analysis of Sun1-GFP Müller glia-derived cells identifies genes differentially regulated by Oct4 overexpression.

Table ST2: Multiomic analysis identifies differentially expressed genes, differential chromatin accessible regions and motif activity along the Müller glia-Bipolar cell neurogenesis trajectory

Table ST3: SnRNA-Seq analysis identifies DEGs induced by Oct4 overexpression in the Müller glia cell clusters from wildtype and *Rbpj*-deficient Müller glia.

Table ST4: SnATAC-Seq analysis identifies differentially accessible chromatin regions regulated by Oct4 overexpression in the Müller glia cell clusters from wildtype and *Rbpj*-deficient Müller glia.

Table ST5: SnATAC-Seq analysis identifies differential motif activity in increased accessible chromatin regions by Oct4 overexpression in the Müller glia cell clusters from wild-type and *Rbpj*-deficient Müller glia.

Table ST6: List of AAV constructs used in the study. Columns identify the AAV construct, titre, and injection volume.

Table ST7: List of antibodies used in the study. Columns identify the antibody, source, catalog number, and RRID identifier.

References:

Abad, María, Lluc Mosteiro, Cristina Pantoja, Marta Cañamero, Teresa Rayon, Inmaculada Ors, Osvaldo Graña, et al. 2013. “Reprogramming in Vivo Produces Teratomas and iPS Cells with Totipotency Features.” *Nature* 502 (7471): 340–45.

Asadi, Sareh, Samaneh Dehghan, Maryam Hajikaram, Seyed Javad Mowla, Abolhassan Ahmadiani Ahmadiani, and Mohammad Javan. 2015. “Comparing The Effects of Small Molecules BIX-01294, Bay K8644, RG-108 and Valproic Acid, and Their Different Combinations on Induction of Pluripotency Marker-Genes by Oct4 in The Mouse Brain.” *Cell Journal* 16 (4): 416–25.

Cebolla, Beatriz, and Mario Vallejo. 2006. “Nuclear Factor-I Regulates Glial Fibrillary Acidic Protein Gene Expression in Astrocytes Differentiated from Cortical Precursor Cells.” *Journal of Neurochemistry* 97 (4): 1057–70.

Chan, Candace S. Y., Nicolas Lonfat, Rong Zhao, Alexander E. Davis, Liang Li, Man-Ru Wu, Cheng-Hui Lin, Zhe Ji, Constance L. Cepko, and Sui Wang. 2020. “Cell Type- and Stage-Specific Expression of Otx2 Is Regulated by Multiple Transcription Factors and -Regulatory Modules in the Retina.” *Development* 147 (14). https://doi.org/10.1242/dev.187922.

Choi, Wonyoung, Mu Seog Choe, Su Min Kim, So Jin Kim, Jiyeon Lee, Yeongun Lee, Sun-Min Lee, So Hee Dho, Min-Young Lee, and Lark Kyun Kim. 2024. “RFX4 Is an Intrinsic Factor for Neuronal Differentiation through Induction of Proneural Genes POU3F2 and NEUROD1.” *Cellular and Molecular Life Sciences: CMLS* 81 (1): 99.

Clark, Brian S., Genevieve L. Stein-O’Brien, Fion Shiau, Gabrielle H. Cannon, Emily Davis-Marcisak, Thomas Sherman, Clayton P. Santiago, et al. 2019. “Single-Cell RNA-Seq Analysis of Retinal Development Identifies NFI Factors as Regulating Mitotic Exit and Late-Born Cell Specification.” *Neuron* 102 (6): 1111–26.e5.

Dehghan, Samaneh, Sareh Asadi, Maryam Hajikaram, Masoud Soleimani, Seyed Javad Mowla, Yaghoub Fathollahi, Abolhassan Ahmadiani, and Mohammad Javan. 2015. “Exogenous Oct4 in Combination with Valproic Acid Increased Neural Progenitor Markers: An Approach for Enhancing the Repair Potential of the Brain.” *Life Sciences* 122 (February):108–15.

Dehghan, S., M. Hesaraki, M. Soleimani, J. Mirnajafi-Zadeh, Y. Fathollahi, and M. Javan. 2016. “Oct4 Transcription Factor in Conjunction with Valproic Acid Accelerates Myelin Repair in Demyelinated Optic Chiasm in Mice.” *Neuroscience* 318 (March):178–89.

Fadl, Benjamin R., Seth A. Brodie, Michael Malasky, Joseph F. Boland, Michael C. Kelly, Matthew W. Kelley, Erich Boger, Robert Fariss, Anand Swaroop, and Laura Campello. 2020. “An Optimized Protocol for Retina Single-Cell RNA Sequencing.” *Molecular Vision* 26 (October):705–17.

Gao, Xiang, Xiaoting Wang, Wenhui Xiong, and Jinhui Chen. 2016. “In Vivo Reprogramming Reactive Glia into iPSCs to Produce New Neurons in the Cortex

Following Traumatic Brain Injury." *Scientific Reports* 6 (March):22490.
Hao, Yuhan, Tim Stuart, Madeline H. Kowalski, Saket Choudhary, Paul Hoffman, Austin Hartman, Avi Srivastava, et al. 2024. "Dictionary Learning for Integrative, Multimodal and Scalable Single-Cell Analysis." *Nature Biotechnology* 42 (2): 293–304.
Hoang, Thanh, Dong Won Kim, Haley Appel, Nicole A. Pannullo, Patrick Leavey, Manabu Ozawa, Sika Zheng, Minzhong Yu, Neal S. Peachey, and Seth Blackshaw. 2022. "Genetic Loss of Function of Ptbp1 Does Not Induce Glia-to-Neuron Conversion in Retina." *Cell Reports* 39 (11): 110849.
Hoang, Thanh, Jie Wang, Patrick Boyd, Fang Wang, Clayton Santiago, Lizhi Jiang, Sooyeon Yoo, et al. 2020. "Gene Regulatory Networks Controlling Vertebrate Retinal Regeneration." *Science* 370 (6519). https://doi.org/10.1126/science.abb8598.
Jorstad, Nikolas L., Matthew S. Wilken, William N. Grimes, Stefanie G. Wohl, Leah S. VandenBosch, Takeshi Yoshimatsu, Rachel O. Wong, Fred Rieke, and Thomas A. Reh. 2017. "Stimulation of Functional Neuronal Regeneration from Müller Glia in Adult Mice." *Nature* 548 (7665): 103–7.
Jorstad, Nikolas L., Matthew S. Wilken, Levi Todd, Connor Finkbeiner, Paul Nakamura, Nicholas Radulovich, Marcus J. Hooper, et al. 2020. "STAT Signaling Modifies Ascl1 Chromatin Binding and Limits Neural Regeneration from Muller Glia in Adult Mouse Retina." *Cell Reports* 30 (7): 2195–2208.e5.
Joung, Julia, Sai Ma, Tristan Tay, Kathryn R. Geiger-Schuller, Paul C. Kirchgatterer, Vanessa K. Verdine, Baolin Guo, et al. 2024. "A Transcription Factor Atlas of Directed Differentiation." *Cell* 187 (12): 3161.
Lengner, Christopher J., G. Grant Welstead, and Rudolf Jaenisch. 2008. "The Pluripotency Regulator Oct4: A Role in Somatic Stem Cells?" *Cell Cycle* 7 (6): 725–28.
Le, Nguyet, Haley Appel, Nicole Pannullo, Thanh Hoang, and Seth Blackshaw. 2022. "Ectopic Insert-Dependent Neuronal Expression of GFAP Promoter-Driven AAV Constructs in Adult Mouse Retina." *Frontiers in Cell and Developmental Biology* 10 (September):914386.
Le, Nguyet, Trieu-Duc Vu, Isabella Palazzo, Ritvik Pulya, Yehna Kim, Seth Blackshaw, and Thanh Hoang. 2024. "Robust Reprogramming of Glia into Neurons by Inhibition of Notch Signaling and Nuclear Factor I (NFI) Factors in Adult Mammalian Retina." *Science Advances* 10 (28): eadn2091.
Loh, Yuin-Han, Qiang Wu, Joon-Lin Chew, Vinsensius B. Vega, Weiwei Zhang, Xi Chen, Guillaume Bourque, et al. 2006. "The Oct4 and Nanog Transcription Network Regulates Pluripotency in Mouse Embryonic Stem Cells." *Nature Genetics* 38 (4): 431–40.
Lyu, Pin, Thanh Hoang, Clayton P. Santiago, Eric D. Thomas, Andrew E. Timms, Haley

Appel, Megan Gimmen, et al. 2021. “Gene Regulatory Networks Controlling Temporal Patterning, Neurogenesis, and Cell-Fate Specification in Mammalian Retina.” *Cell Reports* 37 (7): 109994.

Melo, Jimmy de, Brian S. Clark, Anand Venkataraman, Fion Shiau, Cristina Zibetti, and Seth Blackshaw. 2018. “Ldb1- and Rnf12-Dependent Regulation of Lhx2 Controls the Relative Balance between Neurogenesis and Gliogenesis in the Retina.” *Development* 145 (9). https://doi.org/10.1242/dev.159970.

Melo, Jimmy de, Katsuaki Miki, Amir Rattner, Phil Smallwood, Cristina Zibetti, Karla Hirokawa, Edwin S. Monuki, Peter A. Campochiaro, and Seth Blackshaw. 2012. “Injury-Independent Induction of Reactive Gliosis in Retina by Loss of Function of the LIM Homeodomain Transcription Factor Lhx2.” *Proceedings of the National Academy of Sciences of the United States of America* 109 (12): 4657–62.

Melo, Jimmy de, Cristina Zibetti, Brian S. Clark, Woochang Hwang, Ana L. Miranda-Angulo, Jiang Qian, and Seth Blackshaw. 2016. “Lhx2 Is an Essential Factor for Retinal Gliogenesis and Notch Signaling.” *The Journal of Neuroscience: The Official Journal of the Society for Neuroscience* 36 (8): 2391–2405.

Mo, Alisa, Eran A. Mukamel, Fred P. Davis, Chongyuan Luo, Gilbert L. Henry, Serge Picard, Mark A. Urich, et al. 2015. “Epigenomic Signatures of Neuronal Diversity in the Mammalian Brain.” *Neuron* 86 (6): 1369–84.

Morrison, Gillian M., and Joshua M. Brickman. 2006. “Conserved Roles for Oct4 Homologues in Maintaining Multipotency during Early Vertebrate Development.” *Development* 133 (10): 2011–22.

Nelson, Branden R., Yumi Ueki, Sara Reardon, Mike O. Karl, Sean Georgi, Byron H. Hartman, Deepak A. Lamba, and Thomas A. Reh. 2011. “Genome-Wide Analysis of Müller Glial Differentiation Reveals a Requirement for Notch Signaling in Postmitotic Cells to Maintain the Glial Fate.” *PloS One* 6 (8): e22817.

Niu, Wenze, Tong Zang, Derek K. Smith, Tou Yia Vue, Yuhua Zou, Robert Bachoo, Jane E. Johnson, and Chun-Li Zhang. 2015. “SOX2 Reprograms Resident Astrocytes into Neural Progenitors in the Adult Brain.” *Stem Cell Reports* 4 (5): 780–94.

Niu, Wenze, Tong Zang, Yuhua Zou, Sanhua Fang, Derek K. Smith, Robert Bachoo, and Chun-Li Zhang. 2013. “In Vivo Reprogramming of Astrocytes to Neuroblasts in the Adult Brain.” *Nature Cell Biology* 15 (10): 1164–75.

Ocampo, Alejandro, Pradeep Reddy, Paloma Martinez-Redondo, Aida Platero-Luengo, Fumiyuki Hatanaka, Tomoaki Hishida, Mo Li, et al. 2016. “In Vivo Amelioration of Age-Associated Hallmarks by Partial Reprogramming.” *Cell* 167 (7): 1719–33.e12.

Ohnishi, Kotaro, Katsunori Semi, Takuya Yamamoto, Masahito Shimizu, Akito Tanaka, Kanae Mitsunaga, Keisuke Okita, et al. 2014. “Premature Termination of Reprogramming in Vivo Leads to Cancer Development through Altered Epigenetic Regulation.” *Cell* 156 (4): 663–77.

Păun, Oana, Yu Xuan Tan, Harshil Patel, Stephanie Strohbuecker, Avinash Ghanate, Clementina Cobolli-Gigli, Miriam Llorian Sopena, et al. 2023. “Pioneer Factor ASCL1 Cooperates with the mSWI/SNF Complex at Distal Regulatory Elements to Regulate Human Neural Differentiation.” *Genes & Development* 37 (5-6): 218–42.

Pollak, Julia, Matthew S. Wilken, Yumi Ueki, Kristen E. Cox, Jane M. Sullivan, Russell J. Taylor, Edward M. Levine, and Thomas A. Reh. 2013. “ASCL1 Reprograms Mouse Muller Glia into Neurogenic Retinal Progenitors.” *Development* 140 (12): 2619–31.

Reyes-Aguirre, Luis I., and Monica Lamas. 2016. “Oct4 Methylation-Mediated Silencing As an Epigenetic Barrier Preventing Müller Glia Dedifferentiation in a Murine Model of Retinal Injury.” *Frontiers in Neuroscience* 10 (November):523.

Rizzino, Angie. 2013. “Concise Review: The Sox2-Oct4 Connection: Critical Players in a Much Larger Interdependent Network Integrated at Multiple Levels.” *Stem Cells* 31 (6): 1033–39.

Sharma, Poonam, Shivangi Gupta, Mansi Chaudhary, Soumitra Mitra, Bindia Chawla, Mohammad Anwar Khursheed, and Rajesh Ramachandran. 2019. “Oct4 Mediates Müller Glia Reprogramming and Cell Cycle Exit during Retina Regeneration in Zebrafish.” *Life Science Alliance* 2 (5). https://doi.org/10.26508/lsa.201900548.

Sim, Su-Eon, Soo-Won Park, Sun-Lim Choi, Nam-Kyung Yu, Hyoung-Gon Ko, Deok-Jin Jang, Kyungmin Lee, and Bong-Kiun Kaang. 2011. “Assessment of the Effects of Virus-Mediated Limited Oct4 Overexpression on the Structure of the Hippocampus and Behavior in Mice.” *BMB Reports* 44 (12): 793–98.

Surzenko, Natalia, Tessa Crowl, Amelia Bachleda, Lee Langer, and Larysa Pevny. 2013. “SOX2 Maintains the Quiescent Progenitor Cell State of Postnatal Retinal Muller Glia.” *Development* 140 (7): 1445–56.

Takahashi, Kazutoshi, and Shinya Yamanaka. 2006. “Induction of Pluripotent Stem Cells from Mouse Embryonic and Adult Fibroblast Cultures by Defined Factors.” *Cell* 126 (4): 663–76.

Takashima, Seiji, Michiko Hirose, Narumi Ogonuki, Miki Ebisuya, Kimiko Inoue, Mito Kanatsu-Shinohara, Takashi Tanaka, Eisuke Nishida, Atsuo Ogura, and Takashi Shinohara. 2013. “Regulation of Pluripotency in Male Germline Stem Cells by Dmrt1.” *Genes & Development* 27 (18): 1949–58.

Uhlen, Mathias, Per Oksvold, Linn Fagerberg, Emma Lundberg, Kalle Jonasson, Mattias Forsberg, Martin Zwahlen, et al. 2010. “Towards a Knowledge-Based Human Protein Atlas.” *Nature Biotechnology* 28 (12): 1248–50.

Wang, Chao, Ruben Rabadan Ros, Paloma Martinez-Redondo, Zaijun Ma, Lei Shi, Yuan Xue, Isabel Guillen-Guillen, et al. 2021. “In Vivo Partial Reprogramming of Myofibers Promotes Muscle Regeneration by Remodeling the Stem Cell Niche.” *Nature Communications* 12 (1): 3094.

Wang, Lei-Lei, Carolina Serrano, Xiaoling Zhong, Shuaipeng Ma, Yuhua Zou, and

Chun-Li Zhang. 2021. “Revisiting Astrocyte to Neuron Conversion with Lineage Tracing in Vivo.” *Cell* 184 (21): 5465–81.e16.

Wang, Sui, Cem Sengel, Mark M. Emerson, and Constance L. Cepko. 2014. “A Gene Regulatory Network Controls the Binary Fate Decision of Rod and Bipolar Cells in the Vertebrate Retina.” *Developmental Cell* 30 (5): 513–27.

Wan, Jin, and Daniel Goldman. 2016. “Retina Regeneration in Zebrafish.” *Current Opinion in Genetics & Development* 40 (October):41–47.

Xiao, Dongchang, Kangxin Jin, Suo Qiu, Qiannan Lei, Wanjing Huang, Haiqiao Chen, Jing Su, et al. 2021. “Regeneration of Ganglion Cells for Vision Restoration in Mammalian Retinas.” *Frontiers in Cell and Developmental Biology* 9 (October):755544.

Xie, Ye, Jing Zhou, and Bo Chen. 2022. “Critical Examination of Ptbp1-Mediated Glia-to-Neuron Conversion in the Mouse Retina.” *Cell Reports* 39 (11): 110960.

Yao, Kai, Suo Qiu, Yanbin V. Wang, Silvia J. H. Park, Ethan J. Mohns, Bhupesh Mehta, Xinran Liu, et al. 2018. “Restoration of Vision after de Novo Genesis of Rod Photoreceptors in Mammalian Retinas.” *Nature* 560 (7719): 484–88.

Yu, Ji-Hea, Bae-Geun Nam, Min-Gi Kim, Soonil Pyo, Jung-Hwa Seo, and Sung-Rae Cho. 2021. “Expression of Reprogramming Factor OCT4 Ameliorates Myelination Deficits and Induces Striatal Neuroprotection in Huntington’s Disease.” *Genes* 12 (5). https://doi.org/10.3390/genes12050712.

Zalc, Antoine, Rahul Sinha, Gunsagar S. Gulati, Daniel J. Wesche, Patrycja Daszczuk, Tomek Swigut, Irving L. Weissman, and Joanna Wysocka. 2021. “Reactivation of the Pluripotency Program Precedes Formation of the Cranial Neural Crest.” *Science* 371 (6529). https://doi.org/10.1126/science.abb4776.

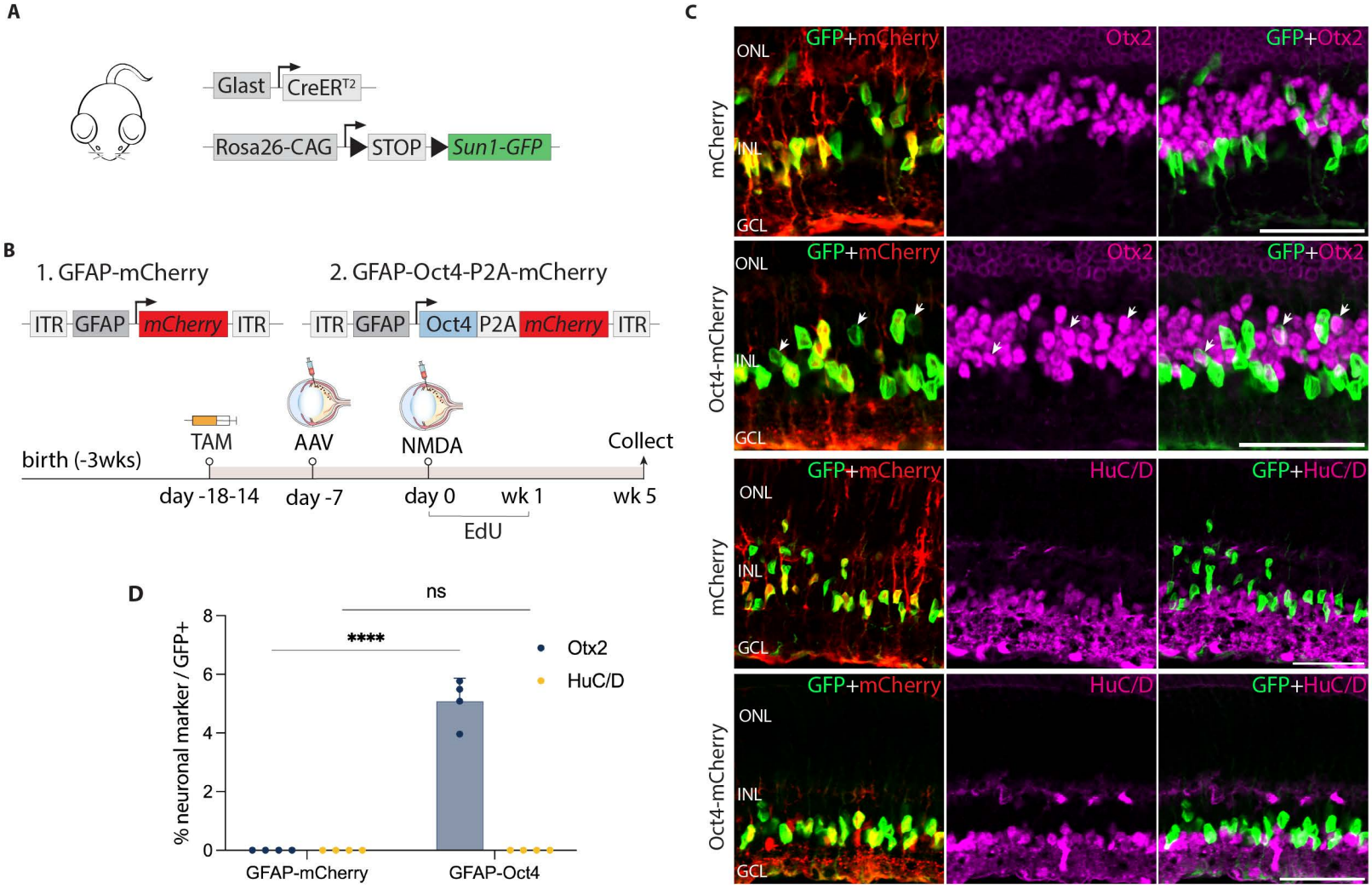
A
Glast
CreER^{T2}
Rosa26-CAG
STOP
Sun1-GFP
B
1. GFAP-mCherry
ITR
GFAP
mCherry
ITR
2. GFAP-Oct4-P2A-mCherry
ITR
GFAP
Oct4
P2A
mCherry
ITR
TAM
AAV
NMDA
Collect
birth (-3wks)
day -18-14
day -7
day 0
wk 1
wk 5
EdU
C
GFP+mCherry
Otx2
GFP+Otx2
HuC/D
GFP+HuC/D
mCherry
Oct4-mCherry
ONL
INL
GCL
D
ns
****
Otx2
HuC/D
% neuronal marker / GFP+
0
2
4
6
8
GFAP-mCherry
GFAP-Oct4

Le *et al.*, Fig. 1

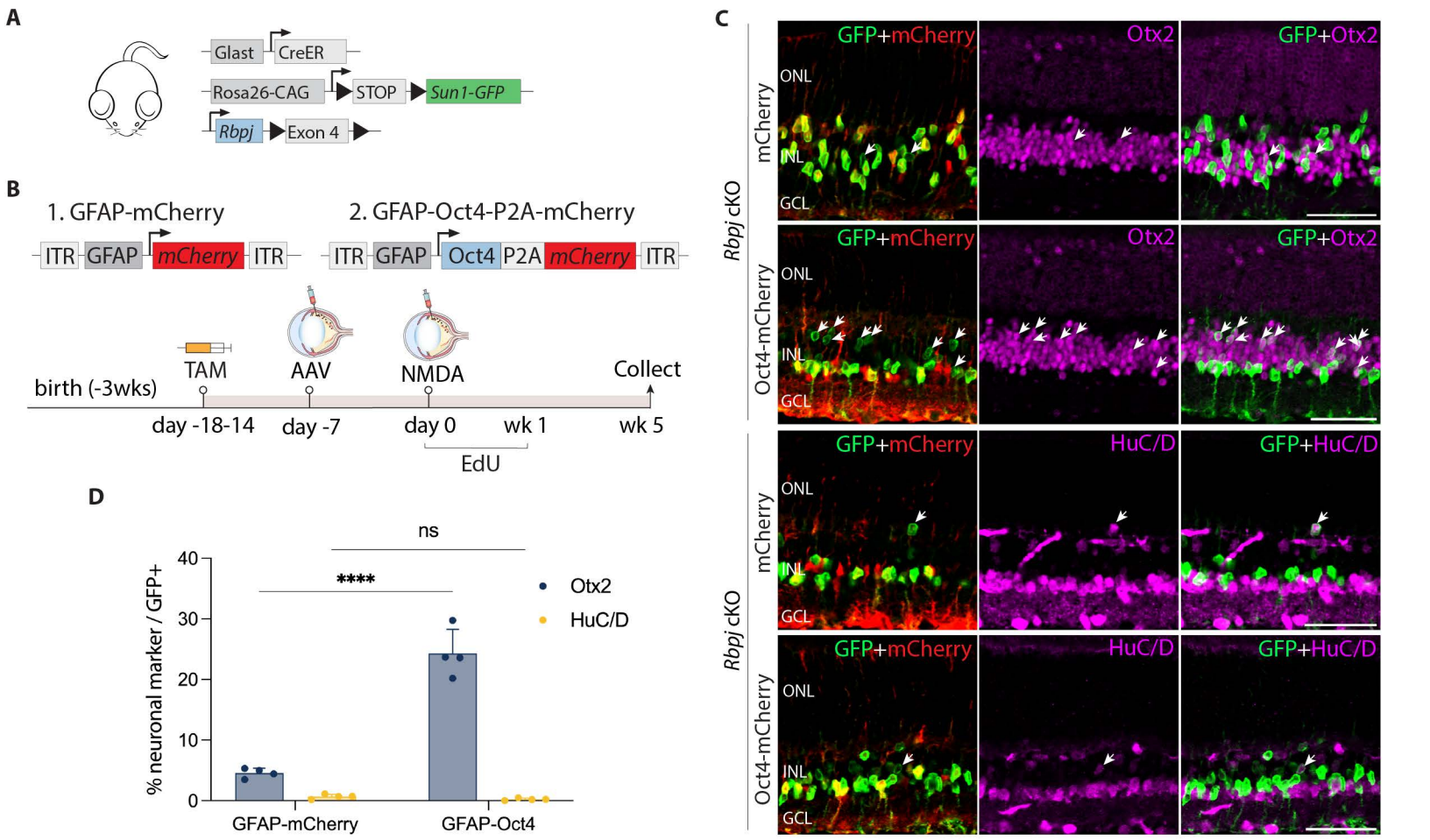
A
Glast
CreER
Rosa26-CAG
STOP
Sun1-GFP
Rbpj
Exon 4
B
1. GFAP-mCherry
ITR
GFAP
mCherry
ITR
2. GFAP-Oct4-P2A-mCherry
ITR
GFAP
Oct4
P2A
mCherry
ITR
TAM
AAV
NMDA
Collect
birth (-3wks)
day -18-14
day -7
day 0
wk 1
wk 5
EdU
D
ns
****
Otx2
HuC/D
% neuronal marker / GFP+
40
30
20
10
0
GFAP-mCherry
GFAP-Oct4
C
Rbpj cKO
mCherry
Oct4-mCherry
GFP+mCherry
Otx2
GFP+Otx2
HuC/D
GFP+HuC/D
ONL
INL
GCL

Le *et al.*, Fig. 2

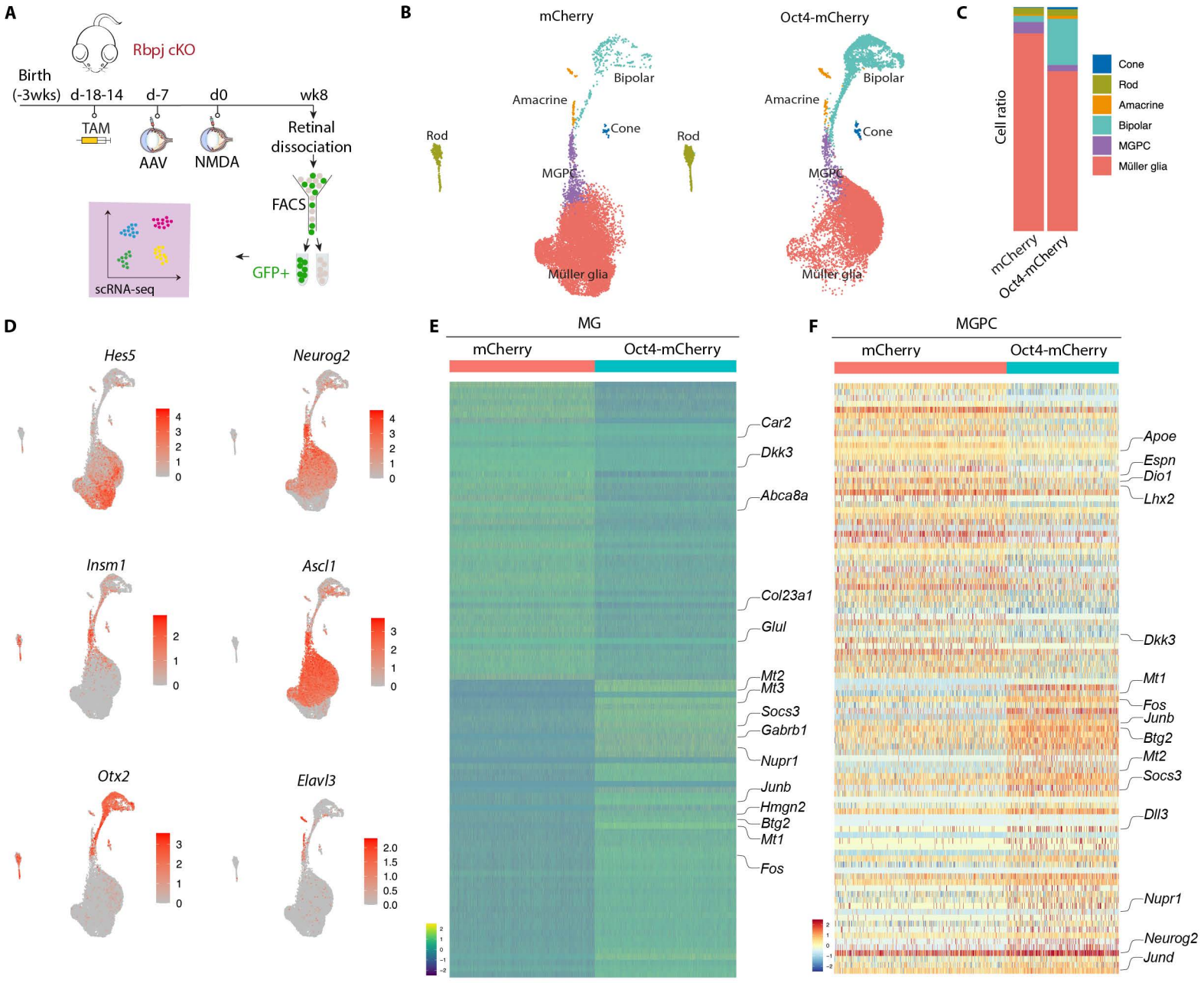
A
Rbpj cKO
Birth
(-3wks)
d-18-14
d-7
d0
wk8
TAM
AAV
NMDA
Retinal dissociation
FACS
GFP+
scRNA-seq
B
mCherry
Oct4-mCherry
Rod
Amacrine
Bipolar
Cone
MGPC
Müller glia
C
Cell ratio
mCherry
Oct4-mCherry
Cone
Rod
Amacrine
Bipolar
MGPC
Müller glia
D
Hes5
Neurog2
Insm1
Ascl1
Otx2
Elavl3
E
MG
mCherry
Oct4-mCherry
Car2
Dkk3
Abca8a
Col23a1
Glul
Mt2
Mt3
Socs3
Gabrb1
Nupr1
Junb
Hmgn2
Btg2
Mt1
Fos
F
MGPC
mCherry
Oct4-mCherry
Apoe
Espn
Dio1
Lhx2
Dkk3
Mt1
Fos
Junb
Btg2
Mt2
Socs3
Dll3
Nupr1
Neurog2
Jund

Le *et al.*, Fig. 3

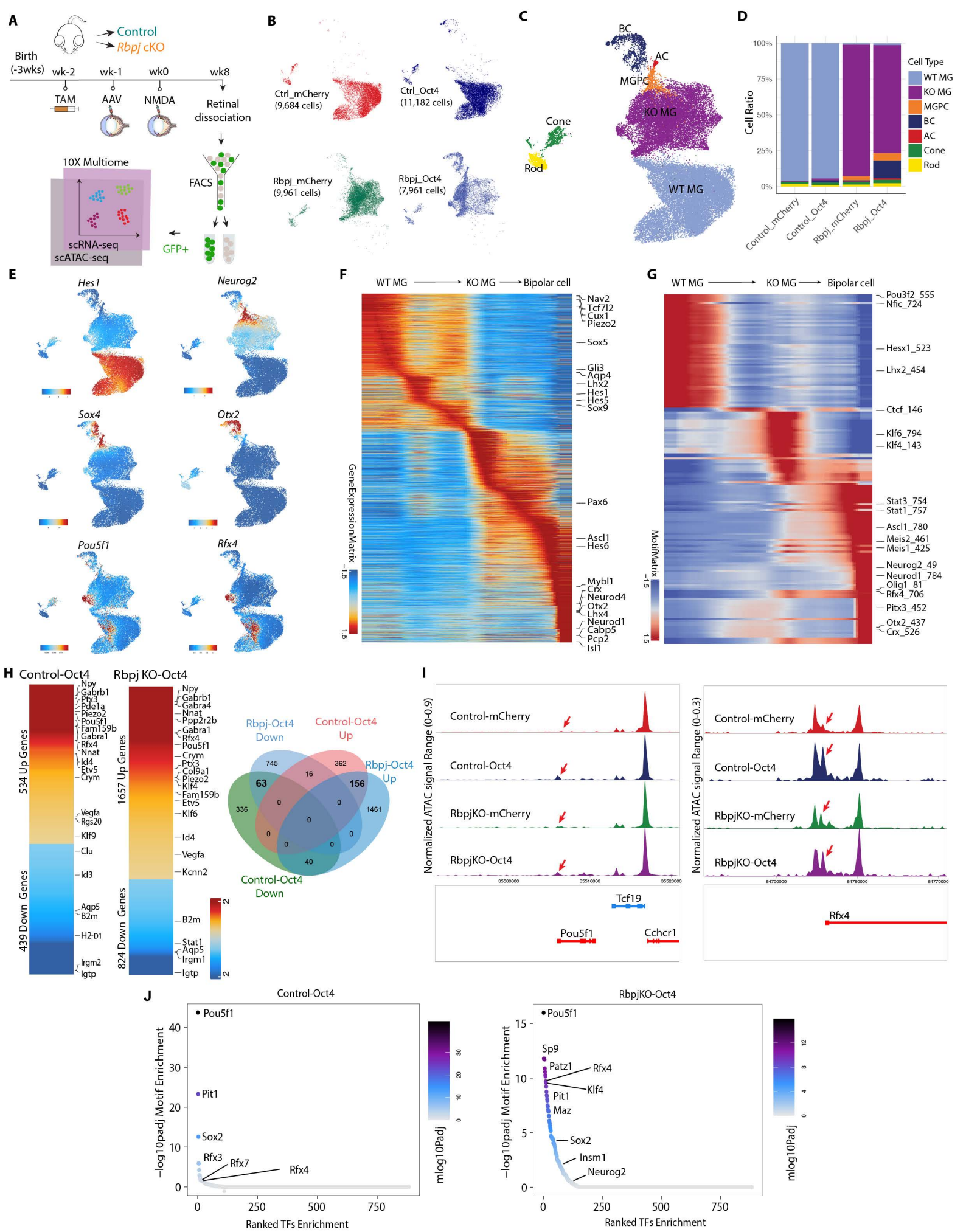
A
Control
Rbpj cKO
Birth
(-3wks)
wk-2
wk-1
wk0
wk8
TAM
AAV
NMDA
Retinal dissociation
FACS
GFP+
10X Multiome
scRNA-seq
scATAC-seq
B
Ctrl_mCherry (9,684 cells)
Ctrl_Oct4 (11,182 cells)
Rbpj_mCherry (9,961 cells)
Rbpj_Oct4 (7,961 cells)
C
BC
AC
MGPC
KO MG
Cone
Rod
WT MG
D
Cell Ratio
100%
75%
50%
25%
0%
Control_mCherry
Control_Oct4
Rbpj_mCherry
Rbpj_Oct4
Cell Type
WT MG
KO MG
MGPC
BC
AC
Cone
Rod
E
Hes1
Neurog2
Sox4
Otx2
Pou5f1
Rfx4
F
WT MG
KO MG
Bipolar cell
GeneExpressionMatrix
Nav2
Tcf7l2
Cux1
Piezo2
Sox5
Gli3
Aqp4
Lhx2
Hes1
Hes5
Sox9
Pax6
Ascl1
Hes6
Mybl1
Crx
Neurod4
Otx2
Lhx4
Neurod1
Cabp5
Pcp2
Isl1
G
WT MG
KO MG
Bipolar cell
MotifMatrix
Pou3f2_555
Nfic_724
Hesx1_523
Lhx2_454
Ctcf_146
Klf6_794
Klf4_143
Stat3_754
Stat1_757
Ascl1_780
Meis2_461
Meis1_425
Neurog2_49
Neurod1_784
Olig1_81
Rfx4_706
Pitx3_452
Otx2_437
Crx_526
H
Control-Oct4
Rbpj KO-Oct4
534 Up Genes
439 Down Genes
1657 Up Genes
824 Down Genes
Npy
Gabrb1
Ptx3
Pde1a
Piezo2
Pou5f1
Fam159b
Gabra1
Rfx4
Nnat
Id4
Etv5
Crym
Vegfa
Rgs20
Klf9
Clu
Id3
Aqp5
B2m
H2-D1
Irgm2
Igtp
Gabra4
Ppp2r2b
Col9a1
Klf4
Klf6
Kcnn2
Stat1
Rbpj-Oct4 Down
Control-Oct4 Up
Rbpj-Oct4 Up
Control-Oct4 Down
745
362
16
63
156
336
1461
40
I
Normalized ATAC signal Range (0-0.9)
Normalized ATAC signal Range (0-0.3)
Control-mCherry
Control-Oct4
RbpjKO-mCherry
RbpjKO-Oct4
Tcf19
Pou5f1
Cchcr1
Rfx4
J
Control-Oct4
RbpjKO-Oct4
−log10padj Motif Enrichment
Ranked TFs Enrichment
mlog10Padj
Pou5f1
Pit1
Sox2
Rfx3
Rfx7
Rfx4
Sp9
Patz1
Klf4
Maz
Insm1
Neurog2

Le *et al.*, Fig. 4

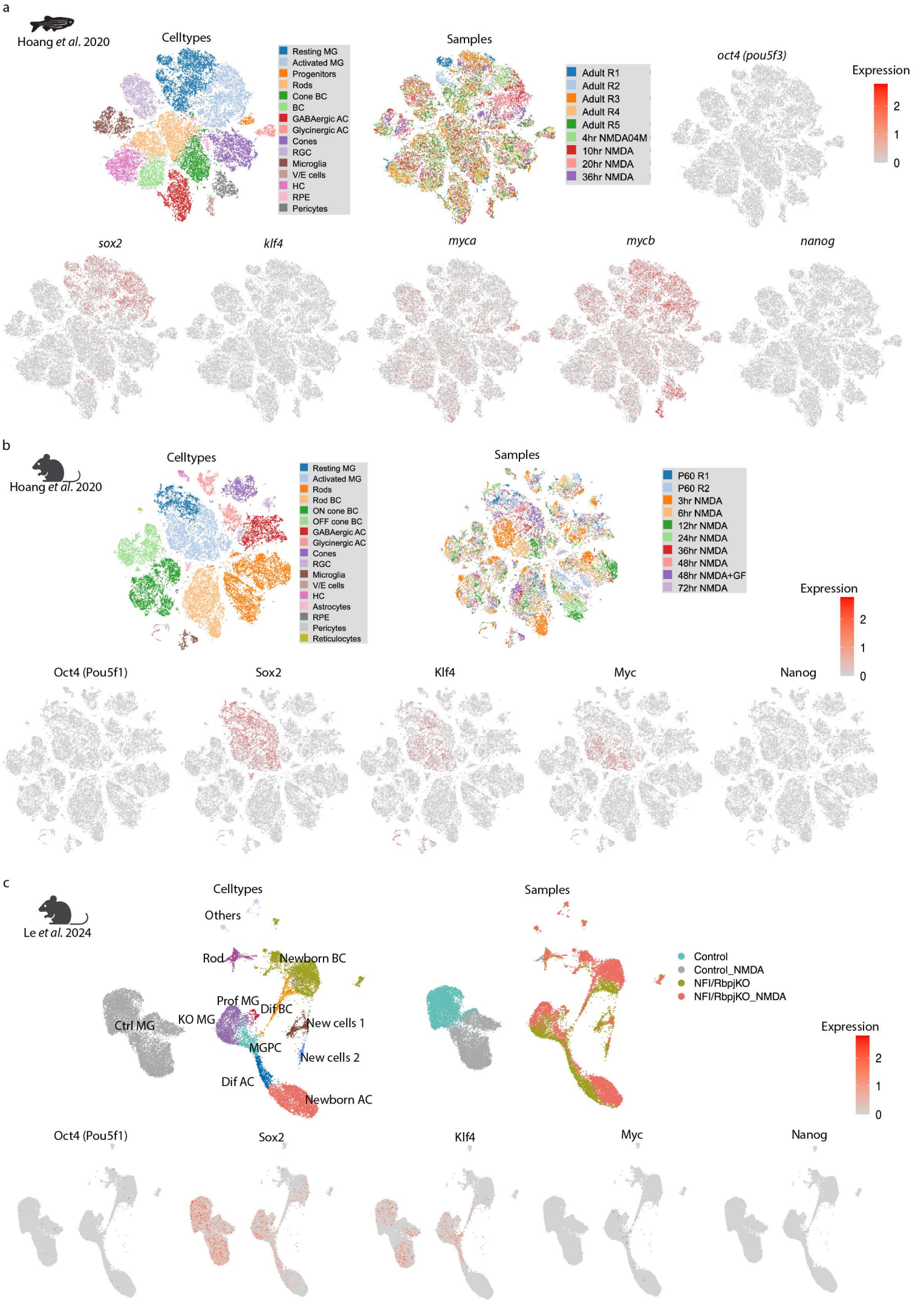

Le *et al.*, Fig. S1

Wildtype

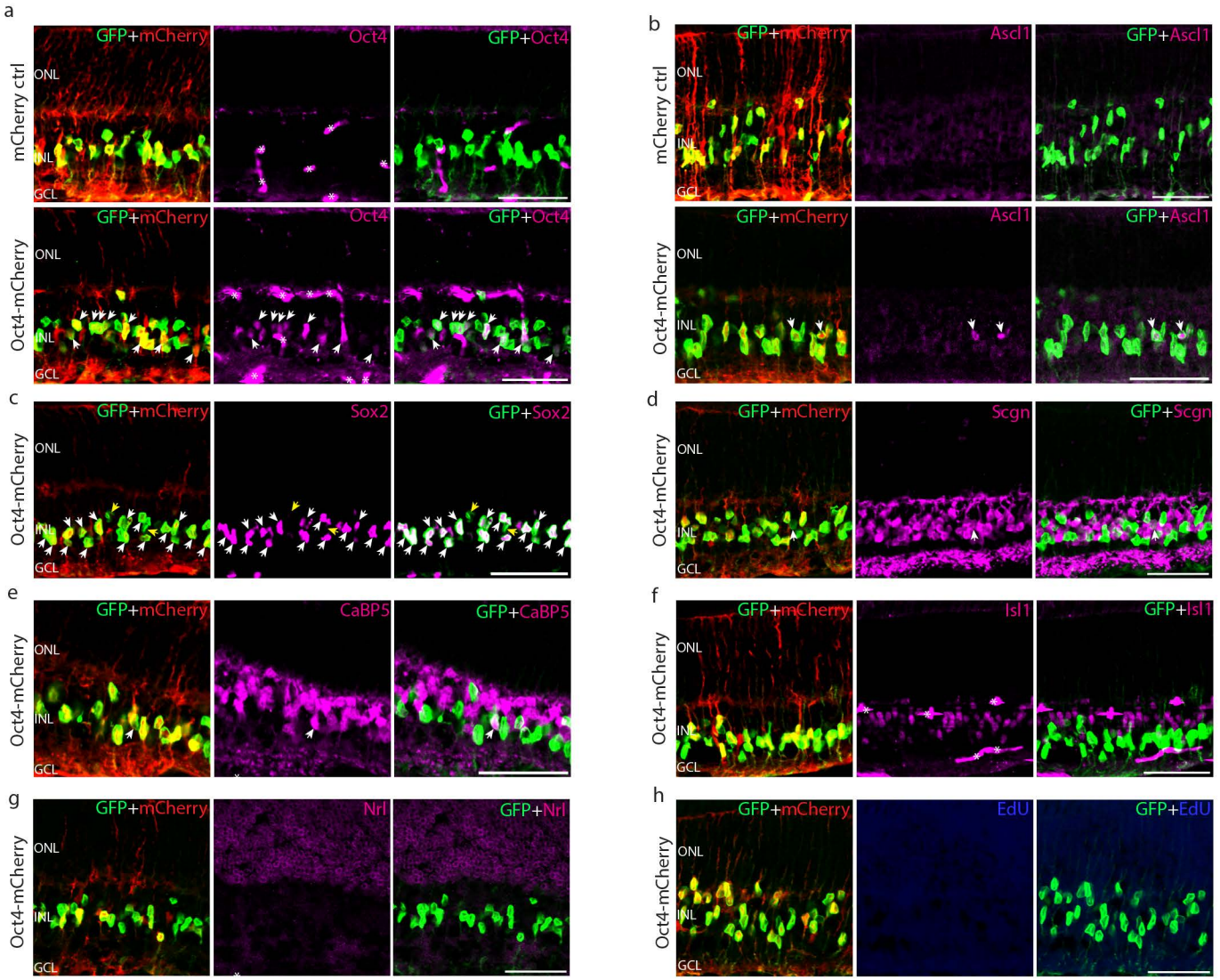

Rbpj cKO

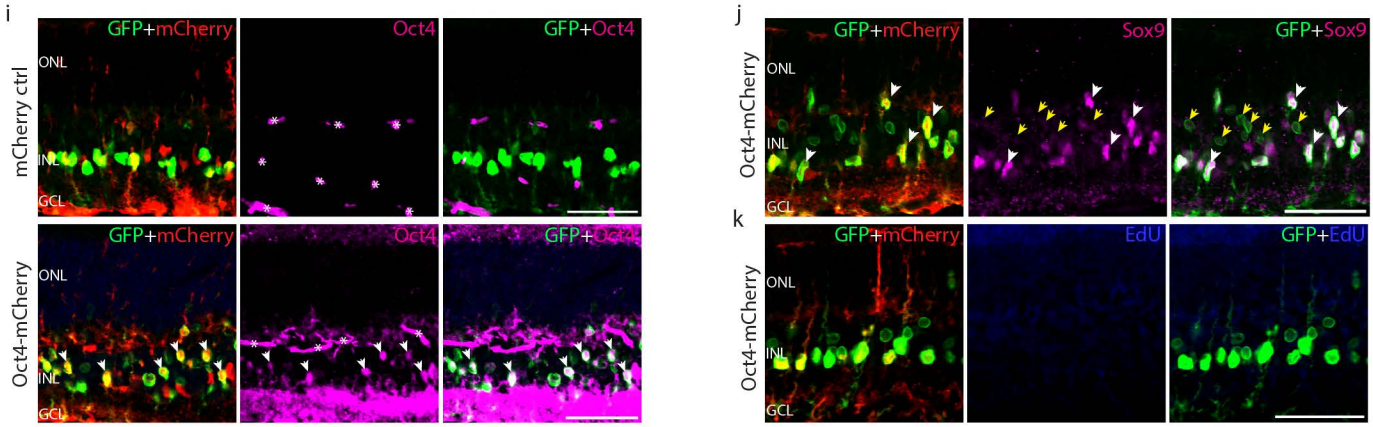

Le *et al.*, Fig. S2

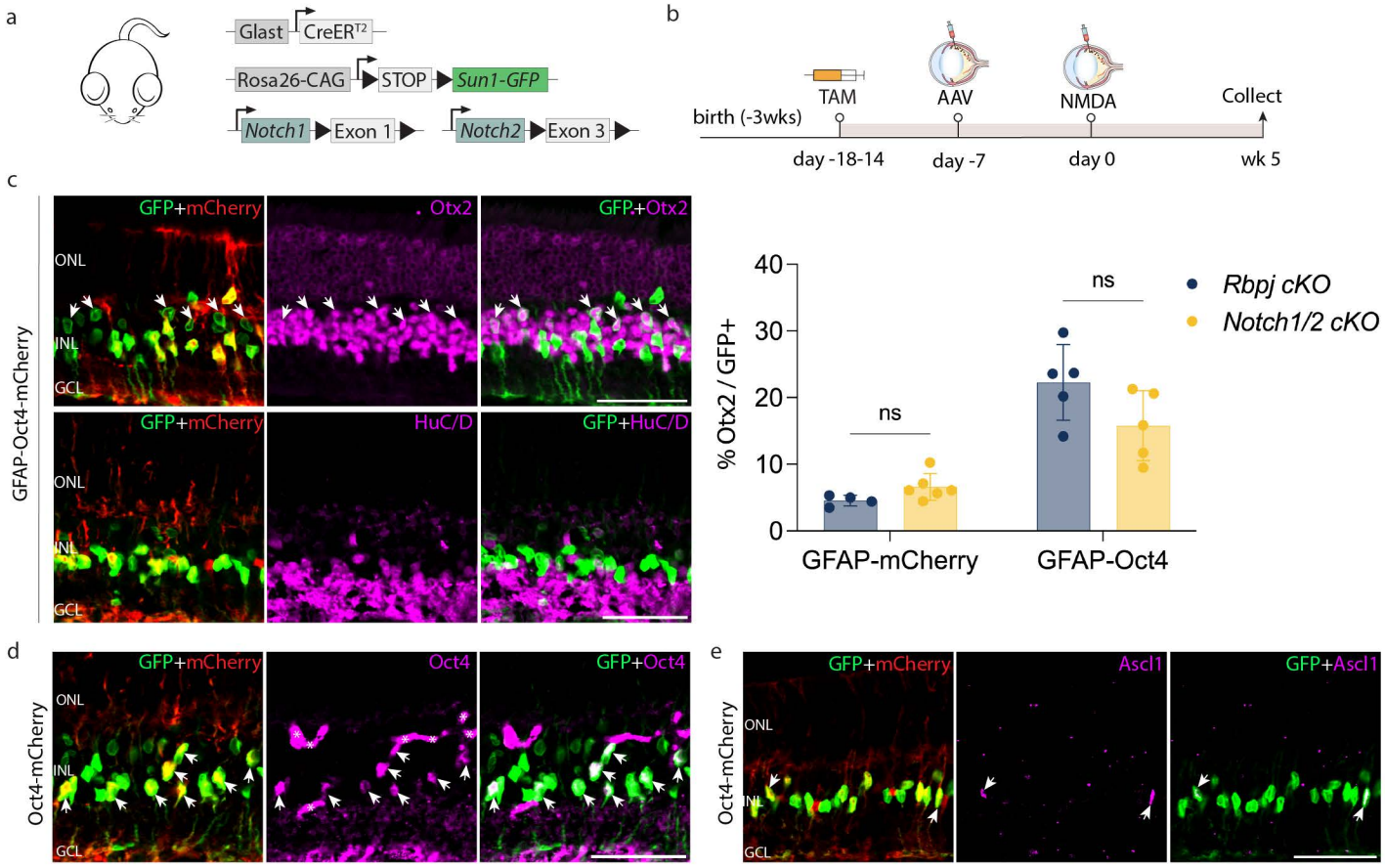

Le *et al.*, Fig. S3

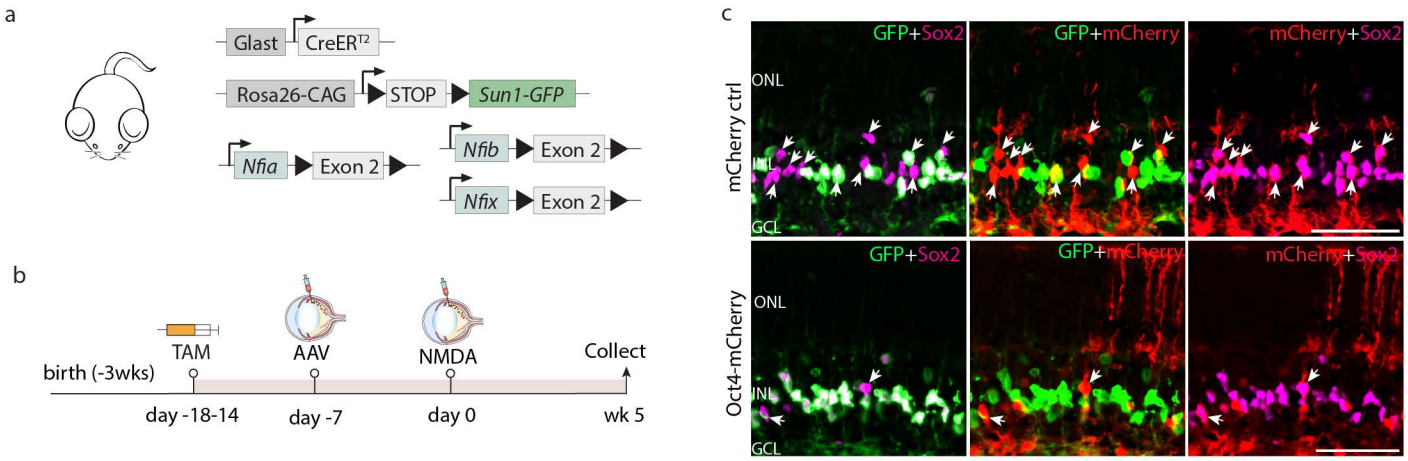

Le *et al.*, Fig. S4

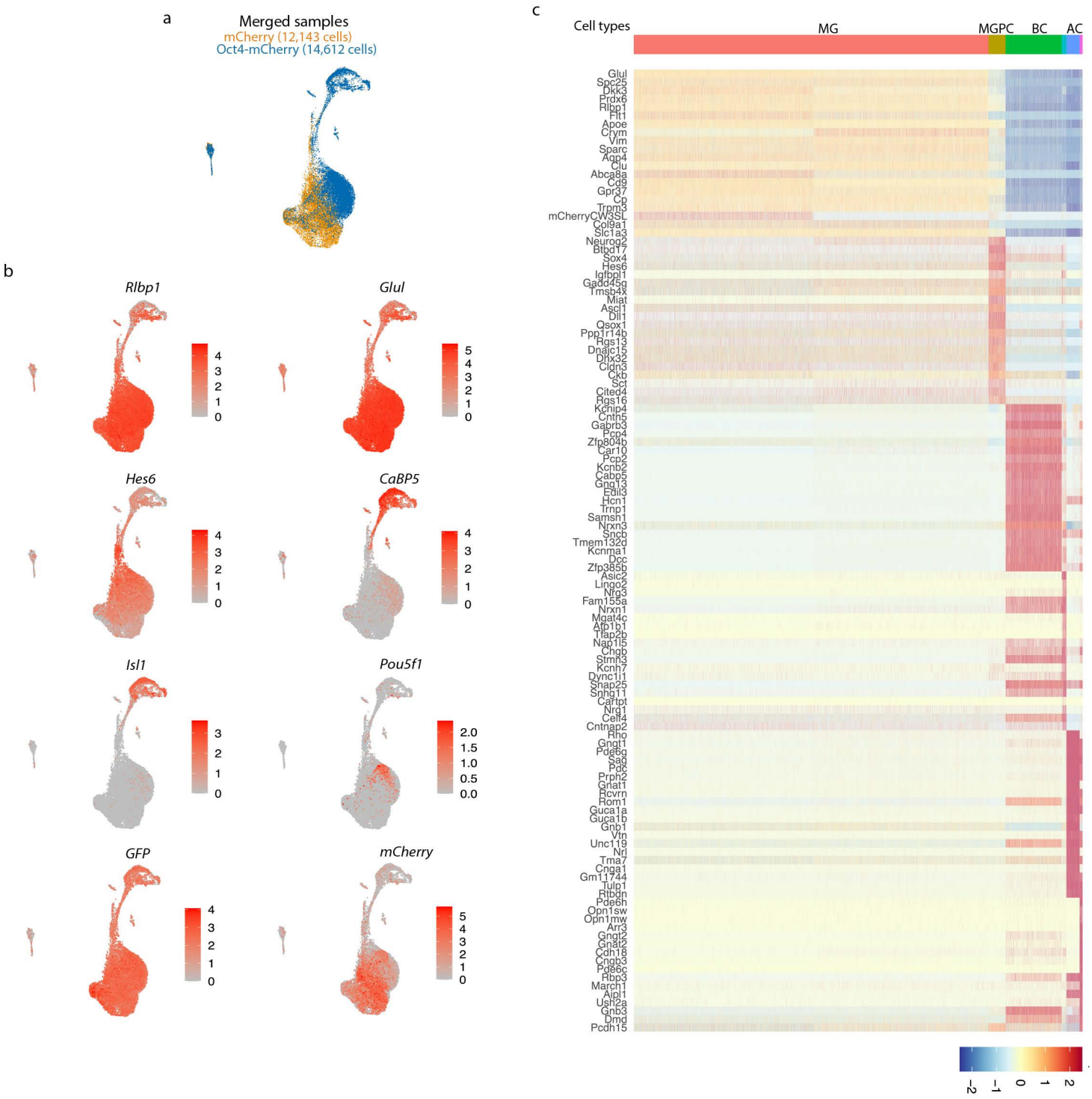

Le *et al.*, Fig. S5

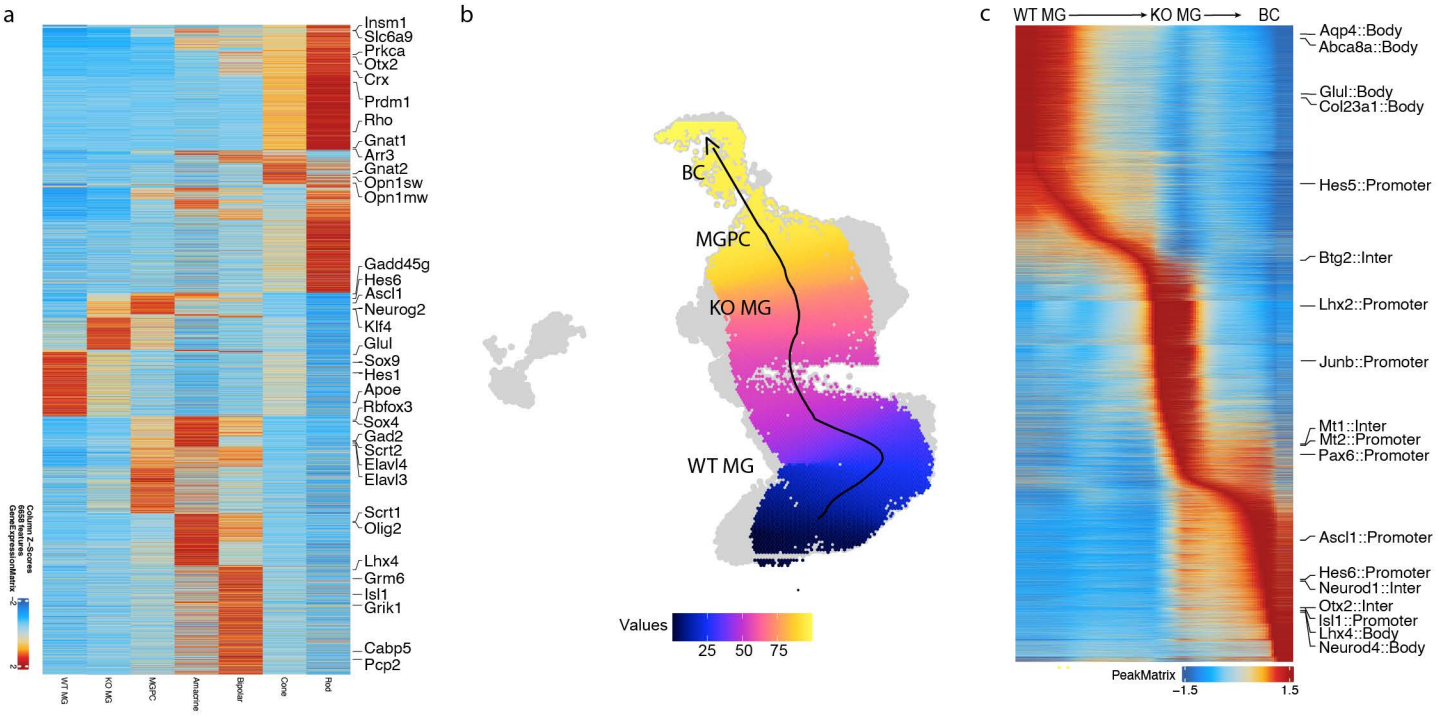

Le *et al.*, Fig. S6